

SELECTIVE CONCEPT BOTTLENECK MODELS WITHOUT PREDEFINED CONCEPTS

Anonymous authors

Paper under double-blind review

ABSTRACT

Concept-based models like Concept Bottleneck Models (CBMs) have garnered significant interest for improving model interpretability by first predicting human-understandable concepts before mapping them to the output classes. Early approaches required costly concept annotations. To alleviate such, recent methods utilized large language models to automatically generate class-specific concept descriptions and learned mappings from a pretrained black-box model’s raw features to these concepts using vision-language models. However, these approaches assume prior knowledge of which concepts the black-box model has learned. In this work, we discover the concepts encoded by the model through unsupervised concept discovery techniques instead. We further propose an input-dependent concept selection mechanism that dynamically retains a sparse set of relevant concepts for each input, enhancing both sparsity and interpretability. Our approach not only improves downstream performance but also needs significantly fewer concepts for accurate classification. Lastly, we show how large vision-language models can guide the editing of our models’ weights to correct errors.

1 INTRODUCTION

Deep neural networks have achieved tremendous success in a variety of tasks on various input modalities. However, they are *black-box* models, making it difficult for humans to understand and comprehend their decisions. Thus, there has been considerable recent interest in developing *interpretable* models. One popular framework is Concept Bottleneck Models (CBMs) (Koh et al., 2020), i.e., models that first predict human-understandable concepts and then use these concepts to predict the classes (Lampert et al., 2009; Kumar et al., 2009). Initial CBMs are trained in an end-to-end fashion through supervision on *both* the concepts and classes. However, the need for human-annotated concepts during model training requires the time-consuming and expensive collection of such.

To address this limitation of initial CBMs, recent work (Yuksekgonul et al., 2023; Oikarinen et al., 2023; Menon & Vondrick, 2023; Marcinkevičs et al., 2024) has proposed converting pretrained black-box models into CBMs in a *post-hoc* fashion. To avoid the need for annotations, they leveraged large language models (e.g., GPT-3 (Brown et al., 2020)) to generate class-specific language descriptions and learned a mapping from the black-box model’s uninterpretable features to these concepts using vision-language models (e.g., CLIP (Radford et al., 2021)). However, this raises a crucial question:

*How can we know **a priori** which concepts a pretrained black-box model has learned?*

Instead of defining the concepts in advance, we propose to discover concepts that accurately decompose the features learned by the black-box model (1st contribution). To do so, we draw from the rich literature on unsupervised concept discovery (Ghorbani et al., 2019; Zhang et al., 2021; Zou et al., 2023; Fel et al., 2023b; Vielhaben et al., 2023; Fel et al., 2023a; Huben et al., 2024; Stein et al., 2024). We chose CRAFT (Fel et al., 2023b) for our experiments because it has been shown to yield human-understandable concepts (Fel et al., 2023a), but other techniques are also possible. CRAFT employs non-negative matrix factorization (Lee & Seung, 1999) to decompose each feature activation into a sparse linear combination of concept vectors. The set of shared concept vectors forms a dictionary matrix. After learning this dictionary matrix, we compute the alignment between the raw bottleneck features and the concept vectors to measure a concept’s presence or absence.

Subsequently, we train an interpretable linear classifier on the concepts’ alignment scores, linking the alignment scores to the predictions. Previous work (Yuksekgonul et al., 2023; Oikarinen et al., 2023) has shown that a sparsity penalty on the linear classifier’s weights ensures that each class relies on only a sparse set of concepts. However, they did not examine the per-sample number of concepts that affect the classification across *all* classes. That is, while individual classes rely on sparse sets of concepts, the overall model depends on substantially more. Empirically, we found that typically over 90% of the available concepts—up to ca. 4200 concepts (see Table 2)—affect the classification per input. As a result, it complicates the interpretation of the model’s decision-making process.

To address these challenges, we propose an *input-dependent concept selection mechanism* that ensures that only a sparse set of concepts relevant for the classification of an individual input sample is dynamically retained (2nd contribution). We simply apply an activation function before the sparse linear classifier, and enforce sparsity on its output or directly use its sparsity parameter. In our experiments, TopK (Makhzani & Frey, 2014) performed best. This mechanism allows the concepts that are retained or removed (i.e., zeroed out) to vary between inputs, making it input-dependent. It also preserves the interpretability of CBMs, as the predictions remain linear w.r.t. the retained concepts.

In summary, our contributions are as follows:

- We propose a new type of CBM called Unsupervised Concept Bottleneck Models (UCBMs)¹; see Figure 1 for an overview. UCBMs convert pretrained, black-box models into a CBM by *discovering and using the concepts that it has learned*.
- We propose a novel input-dependent concept selection mechanism that *dynamically retains a sparse set of concepts* relevant to classification. For example, as few as ca. 1.4% of the available concepts are used per input (Table 2).
- We show that UCBMs improve *performance* while having a substantially higher degree of *sparsity* compared to previous work (Tables 1 and 2).
- We show that UCBMs are *interpretable* qualitatively as well as through a user study (Section 3.2), and demonstrate that large-vision-language models can help us to *intervene* on UCBMs’ weights to fix errors (Section 3.3).

2 UNSUPERVISED CONCEPT BOTTLENECK MODELS WITH INPUT-DEPENDENT CONCEPT SELECTION

In this section, we introduce Unsupervised Concept Bottleneck Models (UCBMs), a novel CBM that uses concepts that are automatically discovered and most accurately decompose features learned by a black-box model (Section 2.1), dynamically only retains the concepts most relevant to classification, and finally classifies the input with a sparse linear model (Section 2.2). Figure 1 provides an overview of UCBMs, and the above steps are described in detail below.

Notations. Let $f : \mathcal{X} \rightarrow \mathbb{R}^p$ be a pretrained, black-box model’s feature extractor that maps from an input space $\mathcal{X} \subseteq \mathbb{R}^d$ to the bottleneck feature space of a size of p . Further, let $\mathbf{X} \in \mathbb{R}^{N \times d}$ be the input data matrix where the i^{th} row is the input $\mathbf{x}_i \in \mathbf{X}$ and let $\mathbf{A} = f(\mathbf{X}) \in \mathbb{R}^{N \times p}$ be the bottleneck feature activations. Lastly, let \mathcal{Y} denote the class label space.

2.1 DISCOVERY OF CONCEPTS LEARNED BY THE BLACK-BOX MODEL

Previous post-hoc CBMs have either used human-annotated concepts (Yuksekgonul et al., 2023; Marcinkevičs et al., 2024) or aligned the black-box model’s features with precomputed text features from vision-language models, using natural language descriptions, such as those generated by a large language model (Yuksekgonul et al., 2023; Oikarinen et al., 2023; Menon & Vondrick, 2023; Marcinkevičs et al., 2024). Importantly, both approaches rely on a *predefined set of concepts*—either through concept annotations or language descriptions thereof—implicitly assuming which concepts the black-box model has learned. However, these concepts are typically unknown in advance.

¹Code is available at <https://anonymous.4open.science/r/ucbm>.

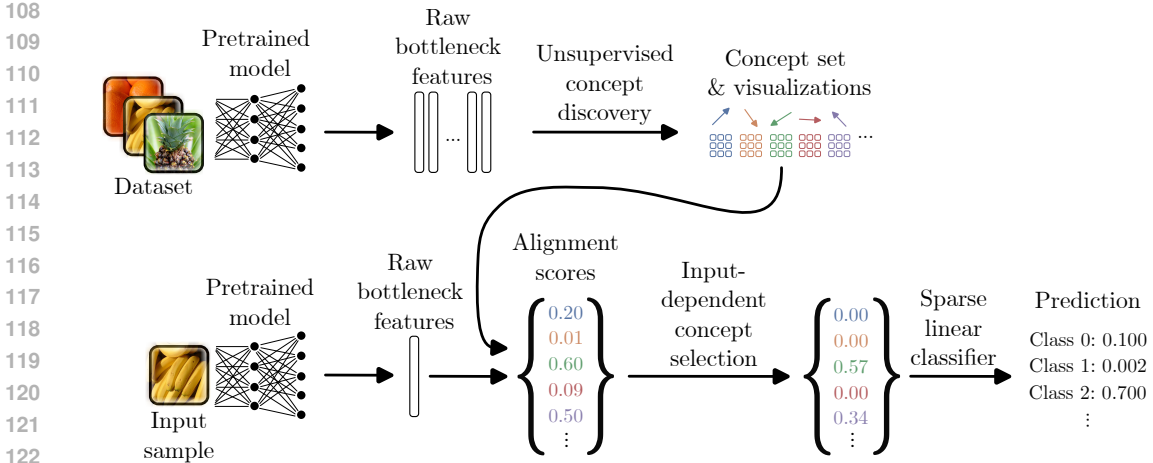


Figure 1: **Overview of Unsupervised Concept Bottleneck Models (UCBMs).** Top: We first extract concepts from raw bottleneck features of a pretrained black-box model using an unsupervised concept discovery method. Bottom: We compute the alignment between the bottleneck’s features and previously discovered concepts (middle). Finally, we train an interpretable classifier consisting of an input-dependent concept selection mechanism and sparse linear classifier (middle to right).

Discovering the concepts that the black-box model has learned. To address this, we propose using unsupervised concept discovery techniques for UCBMs. These enable us to discover the concepts that the black-box model has learned, and do not require defining the concepts in advance.

Formally, the goal of unsupervised concept discovery is to extract a small set of interpretable concepts \mathbf{c} that most faithfully reconstruct the feature activations \mathbf{A} . Assuming linearity of concepts, as per the superposition hypothesis (Kim et al., 2018; Elhage et al., 2022), unsupervised discovery methods can be understood as an instance of a dictionary learning problem (Dumitrescu & Irofti, 2018), as shown by Fel et al. (2023a):

$$(\mathbf{U}^*, \mathbf{C}^*) = \arg \min_{\mathbf{U}, \mathbf{C}} \|\mathbf{A} - \mathbf{UC}\|_F^2, \tag{1}$$

where $\mathbf{U} \in \mathbb{R}^{N \times |\mathbf{C}|}$ (sparse coefficient matrix) represents the activations $\mathbf{A} = f(\mathbf{X}) \in \mathbb{R}^{N \times p}$ w.r.t. a new basis spanned by the set of $|\mathbf{C}|$ concept activation vectors $\mathbf{C} \in \mathbb{R}^{|\mathbf{C}| \times p}$ (dictionary matrix), and $\|\cdot\|_F$ denotes the Frobenius norm. Intuitively, we learn a sparse linear decomposition of the feature activations for each input in Equation 1, where we weigh the shared concepts vectors by the input-specific sparse coefficients. Fel et al. (2023a) showed that previous methods, such as K-Means (Ghorbani et al., 2019), PCA (Zhang et al., 2021; Zou et al., 2023), non-negative matrix factorization (Lee & Seung, 1999; Zhang et al., 2021; Fel et al., 2023b), or sparse autoencoders (Makhzani & Frey, 2014; Huben et al., 2024), only differ in their constraints on \mathbf{U}, \mathbf{C} in Equation 1.

In this work, we chose non-negative matrix factorization (i.e., CRAFT (Fel et al., 2023b)) for UCBMs, as it has been shown to discover human-understandable concepts (Fel et al., 2023a). However, we emphasize that UCBMs will benefit from future unsupervised concept discovery methods.

2.2 LEARNING THE CLASSIFIER WITH INPUT-DEPENDENT CONCEPT SELECTION

In the previous subsection, we discovered concept vectors \mathbf{c}_j that most accurately decompose the uninterpretable features of a black-box model. Next, we compute the alignment scores between each concept vector and the model’s features, denoted as $\text{sim}_{\mathbf{C}}(\mathbf{x}_i) \in [-1, 1]^{|\mathbf{C}|}$, where $\text{sim}_{\mathbf{C}}(\mathbf{x}_i)_j := \frac{\langle \mathbf{a}_i, \mathbf{c}_j \rangle}{\|\mathbf{a}_i\|_2 \|\mathbf{c}_j\|_2}$ is the cosine similarity between the feature activations $\mathbf{a}_i = f(\mathbf{x}_i)$ of input \mathbf{x}_i and concept $\mathbf{c}_j \in \mathbf{C}$. Then, we dynamically select the most relevant concepts and subsequently classify the input with a sparse linear model (Wong et al., 2021). Both are described in detail below.

Sparse linear classifier. Following Yuksekgonul et al. (2023); Oikarinen et al. (2023), we learn a sparse linear classifier by enforcing sparsity on its weight matrix (Wong et al., 2021):

$$\min_{\mathbf{W}, \mathbf{b}} \sum_{i=1}^N \mathcal{L}(\mathbf{W} \text{sim}_{\mathbf{C}}(\mathbf{x}_i) + \mathbf{b}, y_i) + \lambda_w \underbrace{R_{\alpha}(\mathbf{W})}_{\mathcal{L}_{\text{sparsity}}^{\mathbf{W}}} \quad , \quad (2)$$

where $\mathbf{W} \in \mathbb{R}^{|\mathcal{Y}| \times |\mathbf{C}|}$ are the weights, $\mathbf{b} \in \mathbb{R}^{|\mathcal{Y}|}$ is the bias, $y_i \in \mathcal{Y}$ is the target class for input \mathbf{x}_i , \mathcal{L} represents the task-specific loss function (cross-entropy loss throughout this work), λ_w controls the regularization strength on \mathbf{W} , and $R_{\alpha}(\mathbf{W}) := (1 - \alpha)^{\frac{1}{2}} \|\mathbf{W}\|_F + \alpha \|\mathbf{W}\|_{1,1}$ denotes the elastic net regularization (Zou & Hastie, 2005). Note that $\text{sim}_{\mathbf{C}}(\mathbf{x}_i)$ is normalized and frozen during optimization. Importantly, the sparsity aims to make the linear model’s classifications sparse and Yuksekgonul et al. (2023) & Oikarinen et al. (2023) have shown that *an individual class* indeed relies on only a sparse set of concepts.

The main limitation with the approach discussed above is that it fails to produce *globally sparse* classifications. Specifically, most concepts contribute to the classification of any given input, meaning that even if a concept has no impact on one class (e.g., the predicted one), it may still influence others. We consider a concept to be actively contributing if it has a non-zero impact on the output (see Equation 7 for details). When we computed the number of such concepts in above approach, we found that nearly all of them affect the classifications (Table 2). This is because the cosine similarities between the black-box model’s activations and concepts are generally non-zero.² This lack of (global) sparsity limits interpretability and makes it challenging to comprehend a prediction.

Input-dependent concept selection mechanism. To ensure that only few concepts affect classification per input without significant performance sacrifices, we propose a simple yet effective *input-dependent concept selection mechanism*. Specifically, we introduce a concept selector $\pi : \mathbb{R}^{|\mathbf{C}|} \rightarrow \mathbb{R}^{|\mathbf{C}|}$, which takes the alignment scores $\text{sim}_{\mathbf{C}}(\mathbf{x}_i)$ as input and outputs a sparse set of non-zero (i.e., active) concepts and zeroes out the others. We enforce sparsity through a penalty term on concept selector’s output: $\mathcal{L}_{\text{sparsity}}^{\pi} = \|\pi(\cdot)\|_0$. Intuitively, the sparsity penalty $\mathcal{L}_{\text{sparsity}}^{\pi}$ drives the concept selector π to only retain a sparse set of concepts which are important for classifying the input \mathbf{x}_i , as signaled by the task-specific loss \mathcal{L} .

We considered three candidates for the implementation of the input-dependent concept selection mechanism (please refer to Appendix B for further technical details):

- **ReLU:** We define the concept selector using the ReLU activation function as:

$$\pi(\mathbf{x}_i) := \max(0, \text{sim}_{\mathbf{C}}(\mathbf{x}_i) - \mathbf{o}) \text{ with trainable offset parameter } \mathbf{o} \in \mathbb{R}_+^{|\mathbf{C}|} \quad . \quad (3)$$

We apply elastic net regularization on the selector’s output: $\mathcal{L}_{\text{sparsity}}^{\pi} = R_{\alpha}(\pi(\mathbf{x}_i))$.

- **JumpReLU:** We use JumpReLU activation function (Erichson et al., 2019) for concept selection with trainable offset parameter $\mathbf{o} \in \mathbb{R}_+^{|\mathbf{C}|}$ and the Heaviside step function H . We define the concept selector as:

$$\pi(\mathbf{x}_i) := \text{sim}_{\mathbf{C}}(\mathbf{x}_i) \cdot H(\text{sim}_{\mathbf{C}}(\mathbf{x}_i) - \mathbf{o}) = \begin{cases} 0, & \text{sim}_{\mathbf{C}}(\mathbf{x}_i) \leq \mathbf{o} \\ \text{sim}_{\mathbf{C}}(\mathbf{x}_i), & \text{sim}_{\mathbf{C}}(\mathbf{x}_i) > \mathbf{o} \end{cases} \quad . \quad (4)$$

Following Rajamanoharan et al. (2024), we compute the gradients of the *expected* loss using straight-through-estimators (Bengio et al., 2013). We use the following sparsity penalty $\mathcal{L}_{\text{sparsity}}^{\pi} = \sum_j^{|\mathbf{C}|} H(\text{sim}_{\mathbf{C}}(\mathbf{x}_i)_j - \mathbf{o}_j)$. Note that $\mathcal{L}_{\text{sparsity}}^{\pi}$ directly optimizes L0.

- **TopK:** The TopK activation function (Makhzani & Frey, 2014) only keeps the $k \ll |\mathbf{C}|$ concepts with the largest alignment scores and zeroes out the remaining concepts:

$$\pi(\mathbf{x}_i) := \text{TopK}(\text{sim}_{\mathbf{C}}(\mathbf{x}_i) - \mathbf{o}) \text{ with trainable offset parameter } \mathbf{o} \in \mathbb{R}_+^{|\mathbf{C}|} \quad . \quad (5)$$

Note that the sparsity can be directly controlled by k and, thus, $\mathcal{L}_{\text{sparsity}}^{\pi} = 0$.

²While the classifier could technically “turn off” a concept \mathbf{c}_j by setting its associated column vector to the null vector ($\mathbf{W}_{:,j} = 0$), this would effectively reduce the number of concepts and degrades performance, e.g., see Figure 3. Consequently, the sparse linear classifier is unlikely to learn many of such null vectors.

Final interpretable classifier. We obtain the final interpretable classifier by plugging Equation 3, 4, or 5 into Equation 2 together with the respective implementation of $\mathcal{L}_{\text{sparsity}}^{\pi}$:

$$\min_{\mathbf{W}, \mathbf{b}, \mathbf{o}} \sum_{i=1}^N \mathcal{L}(\mathbf{W}\pi(\mathbf{x}_i) + \mathbf{b}, y_i) + \lambda_w \mathcal{L}_{\text{sparsity}}^{\mathbf{W}} + \lambda_{\pi} \mathcal{L}_{\text{sparsity}}^{\pi}, \quad (6)$$

where λ_{π} (or k for TopK) controls the regularization strength of $\mathcal{L}_{\text{sparsity}}^{\pi}$. Appendix B provides a detailed overview for all variants. It is important to note that the selection of concepts is learned in an unsupervised manner, and that the prediction remains linear w.r.t. the *active* concepts ($\pi(\mathbf{x}_i) \neq 0$).

Concept dropout. During initial experiments, we found that models became overly reliant on a single concept. To reduce this reliance, we added a dropout layer (Srivastava et al., 2014) after concept selection. As dropout is applied per concept, it encourages the model to spread its classification decisions across more concepts. Interestingly, we found that this could also improve performance.

3 EXPERIMENTS

We evaluated UCBM on diverse image classification tasks and compared it to relevant baselines. We show that UCBMs outperform prior work and narrow the gap to their black-box counterparts, while relying on substantially fewer concepts globally in their classification (Section 3.1). Then, we demonstrate the interpretability qualitatively as well as through a user study (Section 3.2). Lastly, we showcase how large vision-language models can be leveraged to improve our UCBMs by informing weight editing in order to fix model errors (Section 3.3).

Datasets & backbone black-box models. Following previous work, we evaluated UCBMs on ImageNet (Deng et al., 2009) with a pretrained ResNet-50 V2 (He et al., 2016), CUB (Wah et al., 2011) with ResNet-18 pretrained on CUB³, and Places-365 (Zhou et al., 2017) with ResNet-18 pretrained on Places-365⁴. These datasets cover a diverse set of tasks from standard image classification (ImageNet), fine-grained classification (CUB), to scene recognition (Places-365).

Implementation details. We trained our UCBMs with Adam (Kingma, 2014) and cosine annealing learning rate scheduling (Loshchilov & Hutter, 2017) for 20 epochs. We used a learning rate of 0.001 on ImageNet and Places-365, and 0.01 on CUB; except for the JumpReLU for which we set it to 0.08 on CUB. We set $\alpha = 0.99$ for the elastic net regularization for all variants. We tuned the other hyperparameters (λ_{π} or k , λ_w , and dropout rate) to yield a good trade-off between performance, sparsity, and fair comparability. Refer to Appendix C for the hyperparameters and to Figure 4 and Appendices D and E for the effect of them.

Experimental setup. Since the number of concepts $|C|$ substantially influence downstream performance, we set $|C|$ proportional to the number of classes with various (expansion) factors $\{0.5, 1, 3, 5\}$. All models were trained on a single NVIDIA RTX 2080 GPU and a full training run took from few minutes to a maximum of 1–2 days depending on dataset size and number of concepts $|C|$. We report top-1 accuracy on the standard holdout sets throughout our experiments.

Baselines. We compared our UCBMs to Post-hoc CBM (Yuksekgonul et al., 2023) and Label-free CBM (Oikarinen et al., 2023), as they are the most related to our work. Note that Post-hoc CBM requires concept annotations and is therefore not applicable on ImageNet and Places-365.

Quality of the discovered concepts. Before we evaluated UCBMs, we verified that the discovered concepts behave faithfully. For this, we analyzed the change in cosine similarities between feature activations and concepts after the removal of relevant image parts of a certain concept; see Figure 2 and Appendix A. For example, as we remove the saw blade (concept 1985), the cosine similarity of the aforementioned concept decreases from ca. 0.5 to around 0.25 (Figure 2). We also verified that concepts are semantically consistent and human-understandable, as seen in the top activating crops throughout this paper. Please refer to, e.g., Fel et al. (2023a) for an extensive analysis.

³Provided at <https://github.com/osmr/imgclsmob>.

⁴Provided at <https://github.com/Trustworthy-ML-Lab/Label-free-CBM>.



Figure 2: **The discovered concepts exhibit faithful behavior.** Removing the saw blade (right) from the original image (left) shrinks the alignment score of the respective concept 1985 (blue). Concepts are represented by their most activating crops. Additional results are provided in [Appendix A](#).

Table 1: **UCBMs outperform the baselines and reduce the gap to the original, black-box model.** We report mean top-1 accuracy with standard deviation across three training runs (we kept the discovered concepts fixed). UCBMs used $|\mathcal{C}| = 3000$ (ImageNet), 200 (CUB), and 1825 (Places-365) concepts. Post-hoc CBM used 112 (CUB) concepts and Label-free CBM used 4521 (ImageNet), 212 (CUB), and 2008 (Places-365) concepts after its concept removal step. For fair comparison, we also varied the number of concepts $|\mathcal{C}|$ for UCBMs and [Figure 3](#) shows that UCBMs *Pareto-dominate* the baselines. Lastly, UCBM w/o concept selection slightly outperforms the variants with concept selection, which *trade-off* performance for increased sparsity (see [Table 2](#) and [Appendix D](#)).

Approach	Sparse?	Top-1 test accuracy		
		ImageNet	CUB	Places-365
Original, black-box model	✗	80.9	76.7	53.69
Post-hoc CBM (Yuksekgonul et al., 2023)	(✓)	n/a	58.80*	n/a
Label-free CBM (Oikarinen et al., 2023)	(✓)	78.09	74.38	50.67
UCBM w/o concept selection	(✓)	79.80 ± 0.027	75.15 ± 0.037	52.41 ± 0.028
UCBM with ReLU concept selector	✓	79.07 ± 0.029	74.61 ± 0.128	50.86 ± 0.021
UCBM with JumpReLU concept selector	✓	79.49 ± 0.016	74.57 ± 0.290	51.24 ± 0.019
UCBM with TopK concept selector	✓	79.32 ± 0.009	74.96 ± 0.083	51.20 ± 0.050

*: reported by [Yuksekgonul et al. \(2023\)](#).

3.1 PERFORMANCE AND SPARSITY RESULTS

How do UCBMs perform? [Table 1](#) shows that UCBMs outperform the baseline methods across all datasets. Thereby, they also close the performance gap to the original, black-box model. We also find that UCBMs without concept selection achieve better performance than UCBMs with concept selection. Note that this is expected, as the concept selection variants trade-off performance for more sparsity ([Table 2](#)). We further investigate this trade-off in [Appendix D](#).

We found that performance is strongly influenced by the total number of concepts $|\mathcal{C}|$ used. In [Figure 3](#), we varied the number of concepts to assess this and, as expected, observe that increasing $|\mathcal{C}|$ improves performance. Notably, our UCBMs Pareto-dominate the baselines, confirming that their superiority from [Table 1](#) is not due to the total number of concepts chosen.

How sparse are UCBMs’ decisions? To assess sparsity, we computed the mean number of concepts that actively influence the classification decision per input. We considered concepts with non-zero contribution as actively influencing the classification. Specifically, concept c_j is considered active for the classification of input x_i if

$$\pi(x_i)_j \neq 0 \wedge \exists y_i \in \{1, \dots, |\mathcal{Y}|\} \text{ such that } \mathbf{W}_{y_i, j} \neq 0 \quad . \quad (7)$$

[Table 2](#) shows that UCBMs with concept selection use significantly fewer concepts globally for classification than Label-free CBM or UCBM without concept selection. For example, on ImageNet, UCBM with TopK concept selector uses an average of 42.0 concepts per input (1.4% of the available concepts), while Label-free CBM and UCBM without concept selection use averages of 4238.0 (93.74%) or 3000.0 (100%), respectively. We find similar differences for CUB and Places-365.

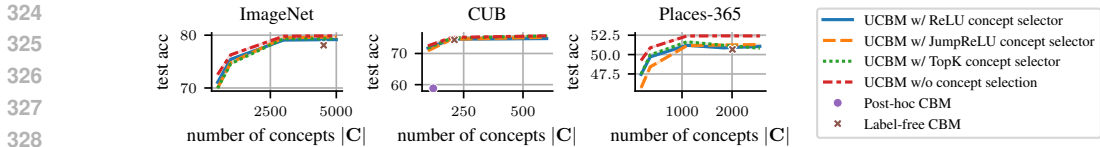


Figure 3: **UCBMs Pareto-dominate the baselines.** We varied the number of available concepts $|C|$. As expected, we found that the more available concepts, the better the downstream performance. Importantly, our UCBMs Pareto-dominate the baseline methods.

Table 2: **The concept selection mechanism leads to substantially fewer concepts being used in the classification.** We report the mean number of active concepts with standard deviation according to Equation 7. Parentheses show their percentage relative to the total number of concepts $|C|$. Label-free CBM and UCBM without input-dependent concept selection use substantially more concepts than our UCBM variants with concept selection.

Approach	Mean number of active concepts (according to Equation 7)		
	ImageNet	CUB	Places-365
Label-free CBM (Oikarinen et al., 2023)	4238.0 ± 0.19 (93.7%)	211.9 ± 0.05 (100%)	1820.0 ± 0.12 (90.6%)
UCBM w/o concept selection	3000.0 ± 0.0 (100%)	200.0 ± 0.0 (100%)	1825.0 ± 0.0 (100%)
UCBM with ReLU concept selector	47.8 ± 0.02 (1.6%)	61.0 ± 0.3 (30.5%)	162.4 ± 0.12 (8.9%)
UCBM with JumpReLU concept selector	42.8 ± 0.07 (1.4%)	62.3 ± 1.13 (31.2%)	166.2 ± 0.94 (9.1%)
UCBM with TopK concept selector	42.0 ± 0.00 (1.4%)	64.2 ± 0.00 (32.1%)	162.0 ± 0.00 (8.9%)

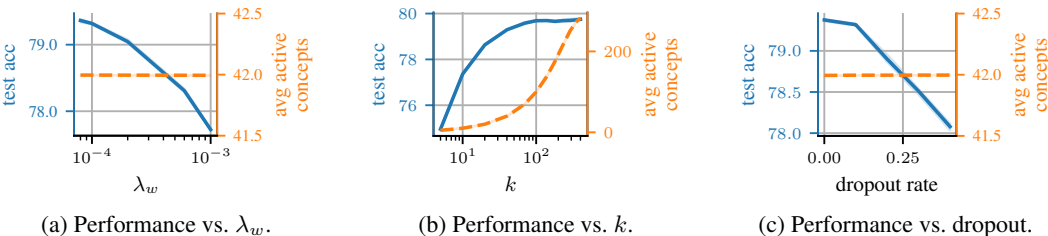


Figure 4: **Sensitivity analysis over λ_w (a), k (b), and dropout (c) on ImageNet.** Larger λ_w and smaller k lead to worse performance. Smaller k leads to higher sparsity. For dropout, there is no clear relation (esp. on the other datasets). Results for the other datasets are provided in Appendix E.

Sensitivity analysis. We varied λ_w (Figure 4a), k (Figure 4b), and dropout rate (Figure 4c) to analyze their impact on performance and sparsity. We find that only k controls sparsity (Equation 7) in TopK, whereas for the other concept selectors, all hyperparameters affect sparsity (see Appendix E). We consider this is as an advantage of TopK, as it disentangles the influence of the hyperparameters. This is discussed in more detail in Appendix E. For performance, we find that larger λ_w and smaller k lead to worse performance. For dropout rate, there typically seems to be a sweet spot.

3.2 INTERPRETABILITY OF UCBM

Explainable sample-wise decisions. Figure 5 shows qualitative examples of the most contributing concepts with their contribution strength (contribution of concept c_j to class $y_i: |\mathbf{W}_{y_i,j}\pi(\mathbf{x}_i)_j|$). We find that the most contributing concepts are relevant to both the input and prediction, while also being diverse. For example, UCBM with TopK concept selector focuses on concepts such as ‘tiger striped fur’, ‘whiskers’ or ‘big cats’ snouts’ for the tiger in Figure 5a, or the ‘bright yellow plumage’ of the American goldfinch in Figure 5b.

Figure 6 compares the explanation of our UCBM with TopK concept selector and Label-free CBM (more examples in Appendix F). We find that UCBM relies on fewer concepts, that are present in the image and relevant to the predicted class. In contrast, Label-free CBM often relies on concepts that are correlated with the predicted class but absent in the image. This is especially pronounced for misclassifications (Figures 17f to 17i in Appendix F).

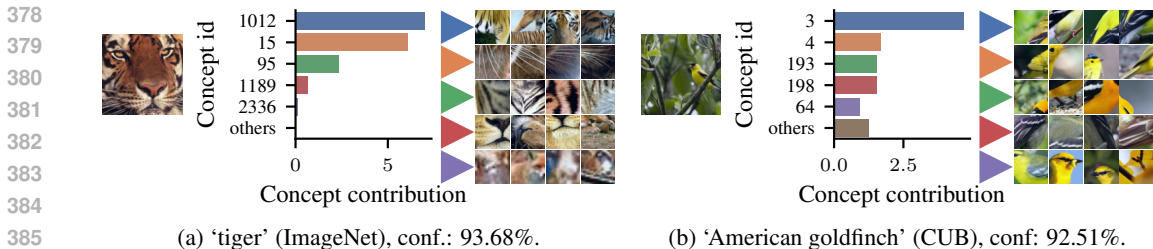


Figure 5: **Decisions of UCBM with TopK concept selector rely on few reasonable and diverse concepts.** Results on ImageNet (a) and CUB (b). Additional examples are provided in Appendix F.

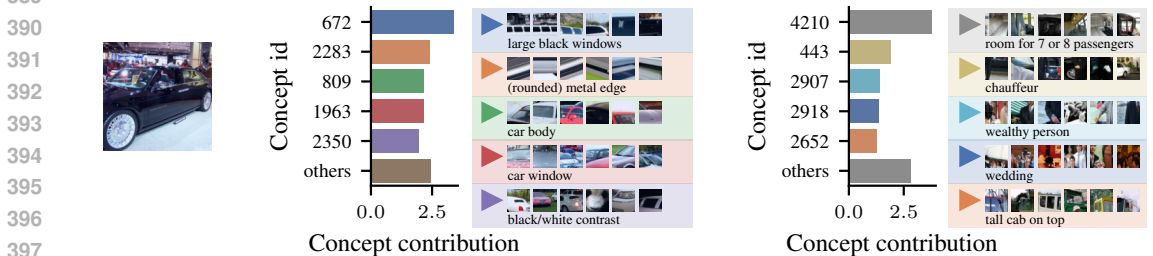


Figure 6: **The decision of UCBM with TopK concept selector (left) is more comprehensible than that of Label-free CBM (right).** Our approach relies on concepts that are present in the image and relevant to the prediction, whereas Label-free CBM tends to use concepts that are not even present, which is particularly pronounced for misclassifications. Appendix F provides additional examples.

User study on explainable sample-wise decisions. To corroborate the qualitative results from above, we conducted a user study to assess the interpretability of UCBM with TopK concept selector compared to Label-free CBM. Specifically, we evaluated the comprehensibility of their explanations. Note that the approaches present their concepts differently: UCBM and Label-free CBM use visual or textual concept representations, respectively. Thus, for fair comparison, we labeled concepts or retrieved images using SigLIP SoViT-400m (Zhai et al., 2023; Alabdulmohsin et al., 2023). Further details on the user study design are provided in Appendix G.

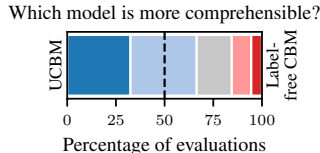


Figure 7: **Users strongly prefer UCBM.** From clearly UCBM (blue) to clearly Label-free CBM (red).

Figure 7 shows that users strongly preferred UCBM over Label-free CBM, corroborating the qualitative results shown in Figures 5 and 6 and Appendix F. Further analysis is provided in Appendix G.

Explainable class-level decision rules. To derive class-level decision rules, we computed the average contribution of each concept for a class. Figure 8 shows the top-3 concepts for two classes. We find that UCBM with TopK concept selector focuses on reasonable, human-understandable concepts relevant to each class. For example, Figure 8a shows that UCBM bases its classification of pineapples on the typical ‘pineapple’s texture’ or its ‘leaves’.

3.3 CASE STUDY: CORRECTING ERRORS USING A LARGE VISION-LANGUAGE MODEL

In this subsection, we show how a large vision-language model (GPT-4o (Achiam et al., 2023)) can guide us to correct errors in UCBMs (specifically, a UCBM with TopK concept selector trained on ImageNet). We prompted the model asking it to adjust the weights of the sparse linear classifier \mathbf{W} in UCBMs (Equation 6) to correct an error without affecting the classification of other inputs. The prompt included the misclassified input image, the top-5 concepts, and their contributions for both the misclassified and correct class. For an example of the prompt, see Appendix J. During initial experiments, we found that the suggested changes, $\Delta \mathbf{W}$, were sometimes too strong, leading to errors of previously correct inputs. To address this, we ran a grid search on the training set of ImageNet to find optimal weighing factors $\beta_i \in [0, 1]$ for each proposed change $\Delta \mathbf{W}_i$.

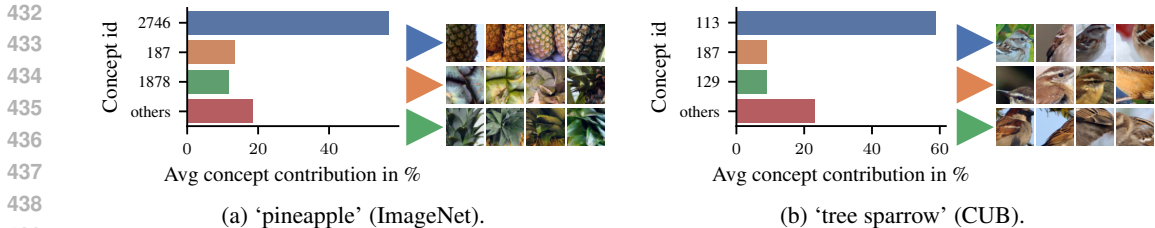


Figure 8: UCBM with TopK concept selector uses concepts that are relevant to the classes (represented by the most activating crops). Results for ImageNet (a) and CUB (b). Additional examples are provided in Appendix H.

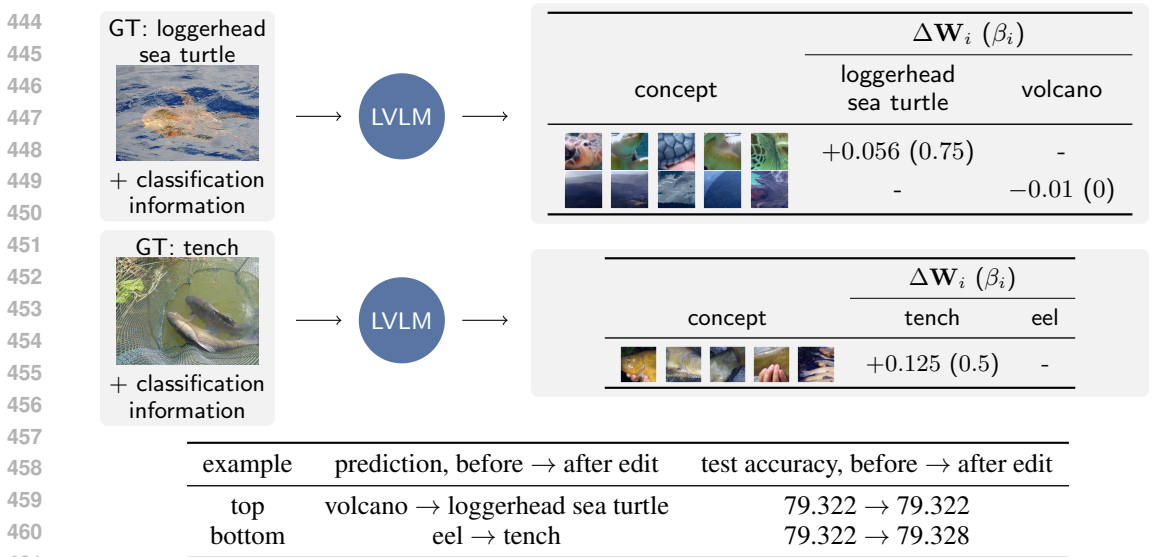


Figure 9: UCBMs are intervenable. We used a large vision-language model to help us to correct errors by guiding the edits of the weights of UCBM with TopK concept selector.

Figure 9 shows two examples that were correctly classified after applying the weight adjustments proposed by the large vision-language model. This demonstrates the intervenability of UCBMs and illustrates the potential use case of large vision-language models to automatically identify and correct the traceable causes of errors of UCBMs (or other concept-based models).

4 RELATED WORKS

Concept-based models. Concept Bottleneck Models (CBMs) (Koh et al., 2020) are trained to directly leverage concepts in their classifications (Lampert et al., 2009; Kumar et al., 2009). Many works highlighted (and partially addressed) the limitations of them (Margeloiu et al., 2021; Mahinpei et al., 2021; Havasi et al., 2022; Marconato et al., 2022; Raman et al., 2024). Other work improved the performance-interpretability trade-off (Espinosa Zarlenga et al., 2022; Yang et al., 2023) or extended them beyond image classification (Ismail et al., 2023; Zarlenga et al., 2023).

The most related methods to our work convert a pretrained black-box model into a CBM post-hoc (Yuksekgonul et al., 2023; Oikarinen et al., 2023; Menon & Vondrick, 2023; Marcinkevics et al., 2024). These approaches alleviate the need for costly concept annotations by leveraging language models, like GPT-3 (Brown et al., 2020), to automatically generate class-specific descriptions and vision-language models, like CLIP (Radford et al., 2021), to learn a mapping from a black-box model’s uninterpretable features to these concepts. In contrast to these, we do not presume which concepts the black-box model has learned, but find the ones that most accurately decompose the black-box model’s features in an unsupervised manner. Concurrently, akin to our first contribution,

Rao et al. (2024) discovered concepts with sparse autoencoders. In contrast to the aforementioned works, we also introduced a novel input-dependent concept selection mechanism that dynamically retains only a sparse set of concepts for each input.

Concept discovery. Early work searched for neuron-aligned concepts (Bau et al., 2017; Olah et al., 2017), while later works, inspired by the superposition hypothesis (Kim et al., 2018; Elhage et al., 2022), went beyond this to (linear) vector (Kim et al., 2018; Zhou et al., 2018; Ghorbani et al., 2019; Zhang et al., 2021; Zou et al., 2023; Fel et al., 2023b; Huben et al., 2024; Stein et al., 2024) or linear subspace (Vielhaben et al., 2023) concept representations. Early work needed costly annotated datasets to find concepts through supervision. Later work overcame this bottleneck by formulating concept discovery as a dictionary learning problem (Fel et al., 2023a).

Model editing. Model editing aims to modify a model’s weights to remove a bias or correct errors. Previous work edited knowledge in large language models (Zhu et al., 2020; Meng et al., 2022), generative image models (Bau et al., 2020; Gandikota et al., 2023), or modified a classifier’s prediction rules (Santurkar et al., 2021; Oikarinen et al., 2023). These works relied on, e.g., human intervention or hypernetworks, whereas we leverage large vision-language models to inform model editing.

5 LIMITATIONS & FUTURE WORK

The main limitation (or advantage) of our approach is that discovered concepts are only represented visually, not textually. While images may be more informative, texts aid faster and easier interpretability. To obtain textual descriptions of concepts, we could manually label concepts. However, this does not scale to large amounts of concepts. Thus, we also experimented with automatic concept labeling through large vision-language models (GPT-4o (Achiam et al., 2023)), see Appendix I for details. While we found it to yield overall good concept descriptions, we also found many instances with poor descriptions; especially for non-object-centric or more abstract concepts.

Another limitation of our approach is that we only extract concepts from the bottleneck layer of black-box models. We conjecture that the use of concepts throughout the feature hierarchy of these models may be beneficial for concept-based models in terms of performance and/or interpretability, as such a hierarchy is also learned by these models (Zeiler & Fergus, 2014). For instance, an early layer could find concepts for ‘windows’, ‘car body’, or ‘wheels’, while a later layer assembles them to a ‘car’ concept (Olah et al., 2020).

6 CONCLUSION

We presented UCBMs, which convert pretrained black-box models into interpretable concept-based models by discovering the concepts that the model has learned through unsupervised concept discovery. We further introduced a novel input-dependent concept selection that only retains the concepts most relevant for classifications. Our experiments show that UCBMs outperform previous methods, while being substantially more sparse globally. Finally, we qualitatively and quantitatively validated the interpretability of UCBMs, and showcased how large vision-language models can guide the editing of UCBMs to correct its errors.

REFERENCES

- 540
541
542 Josh Achiam, Steven Adler, Sandhini Agarwal, Lama Ahmad, Ilge Akkaya, Florencia Leoni Ale-
543 man, Diogo Almeida, Janko Altenschmidt, Sam Altman, Shyamal Anadkat, et al. Gpt-4 technical
544 report. *arXiv*, 2023.
- 545 Ibrahim M Alabdulmohsin, Xiaohua Zhai, Alexander Kolesnikov, and Lucas Beyer. Getting vit in
546 shape: Scaling laws for compute-optimal model design. *Advances in Neural Information Pro-
547 cessing Systems*, 2023.
- 548 David Bau, Bolei Zhou, Aditya Khosla, Aude Oliva, and Antonio Torralba. Network dissection:
549 Quantifying interpretability of deep visual representations. In *Proceedings of the IEEE conference
550 on computer vision and pattern recognition*, pp. 6541–6549, 2017.
- 551 David Bau, Steven Liu, Tongzhou Wang, Jun-Yan Zhu, and Antonio Torralba. Rewriting a deep
552 generative model. In *Computer Vision–ECCV 2020: 16th European Conference, Glasgow, UK,
553 August 23–28, 2020, Proceedings, Part I 16*, pp. 351–369. Springer, 2020.
- 554
555 Yoshua Bengio, Nicholas Léonard, and Aaron Courville. Estimating or propagating gradients
556 through stochastic neurons for conditional computation. *arXiv*, 2013.
- 557 Tom Brown, Benjamin Mann, Nick Ryder, Melanie Subbiah, Jared D Kaplan, Prafulla Dhariwal,
558 Arvind Neelakantan, Pranav Shyam, Girish Sastry, Amanda Askell, Sandhini Agarwal, Ariel
559 Herbert-Voss, Gretchen Krueger, Tom Henighan, Rewon Child, Aditya Ramesh, Daniel Ziegler,
560 Jeffrey Wu, Clemens Winter, Chris Hesse, Mark Chen, Eric Sigler, Mateusz Litwin, Scott Gray,
561 Benjamin Chess, Jack Clark, Christopher Berner, Sam McCandlish, Alec Radford, Ilya Sutskever,
562 and Dario Amodei. Language models are few-shot learners. In *Advances in Neural Information
563 Processing Systems*, 2020.
- 564 Jia Deng, Wei Dong, Richard Socher, Li-Jia Li, Kai Li, and Li Fei-Fei. Imagenet: A large-scale hi-
565 erarchical image database. In *2009 IEEE conference on computer vision and pattern recognition*,
566 pp. 248–255. Ieee, 2009.
- 567
568 Bogdan Dumitrescu and Paul Irofti. *Dictionary learning algorithms and applications*. Springer,
569 2018.
- 570 Nelson Elhage, Tristan Hume, Catherine Olsson, Nicholas Schiefer, Tom Henighan, Shauna Kravec,
571 Zac Hatfield-Dodds, Robert Lasenby, Dawn Drain, Carol Chen, et al. Toy models of superposi-
572 tion. *arXiv*, 2022.
- 573
574 N. Benjamin Erichson, Zhewei Yao, and Michael W. Mahoney. Jumprelu: A retrofit defense strategy
575 for adversarial attacks. *arXiv*, 2019.
- 576 Mateo Espinosa Zarlenga, Pietro Barbiero, Gabriele Ciravegna, Giuseppe Marra, Francesco Gian-
577 nini, Michelangelo Diligenti, Zohreh Shams, Frederic Precioso, Stefano Melacci, Adrian Weller,
578 et al. Concept embedding models: Beyond the accuracy-explainability trade-off. *Advances in
579 Neural Information Processing Systems*, 35:21400–21413, 2022.
- 580
581 Thomas Fel, Victor Boutin, Louis Béthune, Rémi Cadène, Mazda Moayeri, Léo Andéol, Mathieu
582 Chalvidal, and Thomas Serre. A holistic approach to unifying automatic concept extraction and
583 concept importance estimation. *Advances in Neural Information Processing Systems*, 36, 2023a.
- 584
585 Thomas Fel, Agustin Picard, Louis Bethune, Thibaut Boissin, David Vigouroux, Julien Colin, Rémi
586 Cadène, and Thomas Serre. Craft: Concept recursive activation factorization for explainability.
587 In *Proceedings of the IEEE Conference on Computer Vision and Pattern Recognition (CVPR)*,
588 2023b.
- 589 Rohit Gandikota, Joanna Materzynska, Jaden Fiotto-Kaufman, and David Bau. Erasing concepts
590 from diffusion models. In *Proceedings of the IEEE/CVF International Conference on Computer
591 Vision*, pp. 2426–2436, 2023.
- 592
593 Amirata Ghorbani, James Wexler, James Y Zou, and Been Kim. Towards automatic concept-based
explanations. *Advances in neural information processing systems*, 32, 2019.

- 594 Marton Havasi, Sonali Parbhoo, and Finale Doshi-Velez. Addressing leakage in concept bottleneck
595 models. *Advances in Neural Information Processing Systems*, 35:23386–23397, 2022.
- 596
- 597 Kaiming He, Xiangyu Zhang, Shaoqing Ren, and Jian Sun. Deep residual learning for image recog-
598 nition. In *Proceedings of the IEEE conference on computer vision and pattern recognition*, pp.
599 770–778, 2016.
- 600 Robert Huben, Hoagy Cunningham, Logan Riggs Smith, Aidan Ewart, and Lee Sharkey. Sparse
601 autoencoders find highly interpretable features in language models. In *The Twelfth International
602 Conference on Learning Representations*, 2024. URL [https://openreview.net/forum?
603 id=F76bwRSLeK](https://openreview.net/forum?id=F76bwRSLeK).
- 604
- 605 Aya Abdelsalam Ismail, Julius Adebayo, Hector Corrada Bravo, Stephen Ra, and Kyunghyun Cho.
606 Concept bottleneck generative models. In *The Twelfth International Conference on Learning
607 Representations*, 2023.
- 608 Been Kim, Martin Wattenberg, Justin Gilmer, Carrie Cai, James Wexler, Fernanda Viegas, et al.
609 Interpretability beyond feature attribution: Quantitative testing with concept activation vectors
610 (tcav). In *International conference on machine learning*, pp. 2668–2677. PMLR, 2018.
- 611
- 612 Diederik P Kingma. Adam: A method for stochastic optimization. *arXiv*, 2014.
- 613
- 614 Pang Wei Koh, Thao Nguyen, Yew Siang Tang, Stephen Mussmann, Emma Pierson, Been Kim,
615 and Percy Liang. Concept Bottleneck Models. In *International conference on machine learning*.
616 PMLR, 2020.
- 617
- 618 Neeraj Kumar, Alexander C Berg, Peter N Belhumeur, and Shree K Nayar. Attribute and simile
619 classifiers for face verification. In *2009 IEEE 12th international conference on computer vision*,
620 pp. 365–372. IEEE, 2009.
- 621
- 622 Christoph H Lampert, Hannes Nickisch, and Stefan Harmeling. Learning to detect unseen object
623 classes by between-class attribute transfer. In *2009 IEEE conference on computer vision and
624 pattern recognition*, pp. 951–958. IEEE, 2009.
- 625
- 626 Daniel D Lee and H Sebastian Seung. Learning the parts of objects by non-negative matrix factor-
627 ization. *Nature*, 1999.
- 628
- 629 Ilya Loshchilov and Frank Hutter. SGDR: Stochastic gradient descent with warm restarts. In *In-
630 ternational Conference on Learning Representations*, 2017. URL [https://openreview.
631 net/forum?id=Skq89Scxx](https://openreview.net/forum?id=Skq89Scxx).
- 632
- 633 Anita Mahinpei, Justin Clark, Isaac Lage, Finale Doshi-Velez, and Weiwei Pan. Promises and
634 pitfalls of black-box concept learning models. *arXiv*, 2021.
- 635
- 636 Alireza Makhzani and Brendan Frey. K-sparse autoencoders. In *International Conference on Learn-
637 ing Representations*, 2014.
- 638
- 639 Ričards Marcinkevičs, Sonia Laguna, Moritz Vandenheert, and Julia E Vogt. Beyond concept bot-
640 tleneck models: How to make black boxes intervenable? *arXiv*, 2024.
- 641
- 642 Emanuele Marconato, Andrea Passerini, and Stefano Teso. Glancenets: Interpretable, leak-proof
643 concept-based models. *Advances in Neural Information Processing Systems*, 35:21212–21227,
644 2022.
- 645
- 646 Andrei Margeloiu, Matthew Ashman, Umang Bhatt, Yanzhi Chen, Mateja Jamnik, and Adrian
647 Weller. Do concept bottleneck models learn as intended? *arXiv*, 2021.
- 648
- 649 Kevin Meng, David Bau, Alex Andonian, and Yonatan Belinkov. Locating and editing factual
650 associations in gpt. *Advances in Neural Information Processing Systems*, 2022.
- 651
- 652 Sachit Menon and Carl Vondrick. Visual classification via description from large language models.
653 In *The Eleventh International Conference on Learning Representations*, 2023. URL [https://
654 openreview.net/forum?id=j1AjNL8z5cs](https://openreview.net/forum?id=j1AjNL8z5cs).

- 648 Tuomas Oikarinen, Subhro Das, Lam M. Nguyen, and Tsui-Wei Weng. Label-free Concept Bot-
649 tleneck Models. In *The Eleventh International Conference on Learning Representations, 2023*.
650 URL <https://openreview.net/forum?id=F1Cg47MNvBA>.
651
- 652 Chris Olah, Alexander Mordvintsev, and Ludwig Schubert. Feature visualization. *Distill*, 2(11):e7,
653 2017.
- 654 Chris Olah, Nick Cammarata, Ludwig Schubert, Gabriel Goh, Michael Petrov, and Shan Carter.
655 Zoom in: An introduction to circuits. *Distill*, 5(3):e00024–001, 2020.
656
- 657 Alec Radford, Jong Wook Kim, Chris Hallacy, Aditya Ramesh, Gabriel Goh, Sandhini Agarwal,
658 Girish Sastry, Amanda Askell, Pamela Mishkin, Jack Clark, et al. Learning transferable visual
659 models from natural language supervision. In *International conference on machine learning*, pp.
660 8748–8763. PMLR, 2021.
- 661 Senthoran Rajamanoharan, Tom Lieberum, Nicolas Sonnerat, Arthur Conmy, Vikrant Varma, János
662 Kramár, and Neel Nanda. Jumping Ahead: Improving Reconstruction Fidelity with JumpReLU
663 Sparse Autoencoders. *arXiv*, 2024.
664
- 665 Naveen Raman, Mateo Espinosa Zarlenga, Juyeon Heo, and Mateja Jamnik. Do concept bottleneck
666 models obey locality? *arXiv*, 2024.
667
- 668 Sukrut Rao, Sweta Mahajan, Moritz Böhle, and Bernt Schiele. Discover-then-name: Task-agnostic
669 concept bottlenecks via automated concept discovery. *arXiv*, 2024.
- 670 Shibani Santurkar, Dimitris Tsipras, Mahalaxmi Elango, David Bau, Antonio Torralba, and Alek-
671 sander Madry. Editing a classifier by rewriting its prediction rules. *Advances in Neural Informa-
672 tion Processing Systems*, 34:23359–23373, 2021.
673
- 674 Nitish Srivastava, Geoffrey Hinton, Alex Krizhevsky, Ilya Sutskever, and Ruslan Salakhutdinov.
675 Dropout: a simple way to prevent neural networks from overfitting. *The journal of machine
676 learning research*, 15(1):1929–1958, 2014.
- 677 Adam Stein, Aaditya Naik, Yinjun Wu, Mayur Naik, and Eric Wong. Towards compositionality in
678 concept learning. In *Forty-first International Conference on Machine Learning, 2024*.
679
- 680 Johanna Vielhaben, Stefan Bluecher, and Nils Strodthoff. Multi-dimensional concept discovery
681 (MCD): A unifying framework with completeness guarantees. *Transactions on Machine Learn-
682 ing Research*, 2023. ISSN 2835-8856. URL <https://openreview.net/forum?id=KxBQpz7HKh>.
683
- 684 Catherine Wah, Steve Branson, Peter Welinder, Pietro Perona, and Serge Belongie. The caltech-ucsd
685 birds-200-2011 dataset, 2011.
686
- 687 Eric Wong, Shibani Santurkar, and Aleksander Madry. Leveraging sparse linear layers for de-
688 buggable deep networks. In *International Conference on Machine Learning*, pp. 11205–11216.
689 PMLR, 2021.
- 690 Yue Yang, Artemis Panagopoulou, Shenghao Zhou, Daniel Jin, Chris Callison-Burch, and Mark
691 Yatskar. Language in a bottle: Language model guided concept bottlenecks for interpretable im-
692 age classification. In *Proceedings of the IEEE/CVF Conference on Computer Vision and Pattern
693 Recognition*, pp. 19187–19197, 2023.
694
- 695 Mert Yuksekgonul, Maggie Wang, and James Zou. Post-hoc Concept Bottleneck Models. In
696 *The Eleventh International Conference on Learning Representations, 2023*. URL <https://openreview.net/forum?id=nA5AZ8CEyow>.
697
- 698 Mateo Espinosa Zarlenga, Zohreh Shams, Michael Edward Nelson, Been Kim, and Mateja Jamnik.
699 TabCBM: Concept-based interpretable neural networks for tabular data. *Transactions on Machine
700 Learning Research*, 2023. ISSN 2835-8856. URL <https://openreview.net/forum?id=TIIsrnWpjQ0>.
701

702 Matthew D Zeiler and Rob Fergus. Visualizing and understanding convolutional networks. In
703 *Computer Vision–ECCV 2014: 13th European Conference, Zurich, Switzerland, September 6-12,*
704 *2014, Proceedings, Part I 13*, pp. 818–833. Springer, 2014.

705 Xiaohua Zhai, Basil Mustafa, Alexander Kolesnikov, and Lucas Beyer. Sigmoid loss for language
706 image pre-training. In *Proceedings of the IEEE/CVF International Conference on Computer*
707 *Vision*, 2023.

708 Ruihan Zhang, Prashan Madumal, Tim Miller, Krista A Ehinger, and Benjamin IP Rubinstein. In-
709 vertible concept-based explanations for cnn models with non-negative concept activation vectors.
710 In *Proceedings of the AAAI Conference on Artificial Intelligence*, pp. 11682–11690, 2021.

711 Bolei Zhou, Agata Lapedriza, Aditya Khosla, Aude Oliva, and Antonio Torralba. Places: A 10
712 million image database for scene recognition. *IEEE transactions on pattern analysis and machine*
713 *intelligence*, 40(6):1452–1464, 2017.

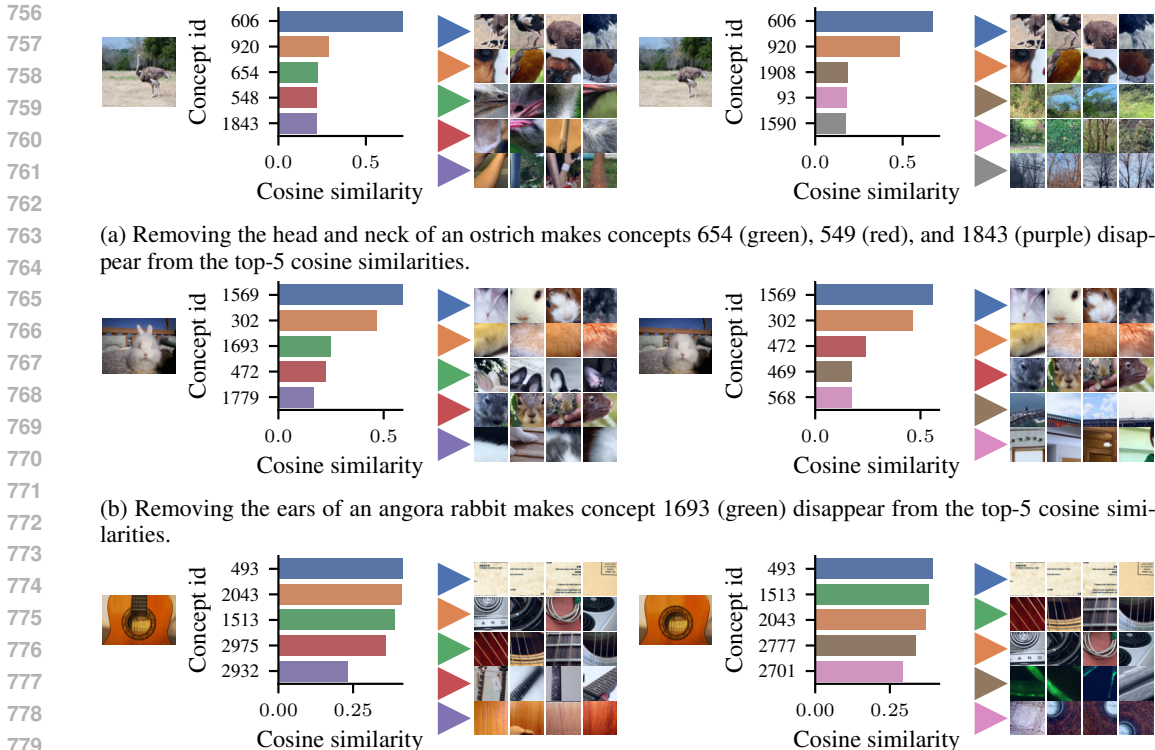
714 Bolei Zhou, Yiyou Sun, David Bau, and Antonio Torralba. Interpretable basis decomposition for
715 visual explanation. In *Proceedings of the European Conference on Computer Vision (ECCV)*, pp.
716 119–134, 2018.

717 Chen Zhu, Ankit Singh Rawat, Manzil Zaheer, Srinadh Bhojanapalli, Daliang Li, Felix Yu, and
718 Sanjiv Kumar. Modifying memories in transformer models. *arXiv*, 2020.

719 Andy Zou, Long Phan, Sarah Chen, James Campbell, Phillip Guo, Richard Ren, Alexander
720 Pan, Xuwang Yin, Mantas Mazeika, Ann-Kathrin Dombrowski, Shashwat Goel, Nathaniel Li,
721 Michael J. Byun, Zifan Wang, Alex Mallen, Steven Basart, Sanmi Koyejo, Dawn Song, Matt
722 Fredrikson, Zico Kolter, and Dan Hendrycks. Representation engineering: A top-down approach
723 to ai transparency, 2023.

724 Hui Zou and Trevor Hastie. Regularization and variable selection via the elastic net. *Journal of the*
725 *Royal Statistical Society Series B: Statistical Methodology*, 67(2):301–320, 2005.

726
727
728
729
730
731
732
733
734
735
736
737
738
739
740
741
742
743
744
745
746
747
748
749
750
751
752
753
754
755



(a) Removing the head and neck of an ostrich makes concepts 654 (green), 549 (red), and 1843 (purple) disappear from the top-5 cosine similarities.

(b) Removing the ears of an angora rabbit makes concept 1693 (green) disappear from the top-5 cosine similarities.

(c) Removing the neck of an acoustic guitar makes concept 2975 (red) disappear from the top-5 cosine similarities.

Figure 10: Concepts discovered in an unsupervised manner exhibit faithful behavior. Concepts are represented by their most activating image crops. From the original image (left), we manually removed image parts (right) using an image manipulation tool and computed the concept-activation cosine similarities for an ostrich (a), an angora rabbit (b), and an acoustic guitar (c). We find that cosine similarity scores reduce, as we remove an image part where that concept or these concepts were previously present.

A ADDITIONAL RESULTS FOR THE FAITHFULNESS OF DISCOVERED CONCEPTS

Figure 10 provides additional results for the faithfulness of the discovered concepts. In Figure 10a removing the head and neck of the ostrich in the input image makes concepts 654 (green), 549 (red), and 1843 (purple) disappear from the top-5 cosine similarities. Since concepts 654, 549 and 1843 represent parts of an ostrich’s head or neck, this demonstrates the faithfulness of the discovered concepts. Figures 10b and 10c show similar behavior for a rabbit’s ears and guitar’s neck, respectively

B FURTHER DETAILS ON THE INTERPRETABLE CLASSIFIERS

Table 3 provides the full overview over the interpretable classifiers for all of our UCBM variants from Section 2.2. Below, we provide further details for the JumpReLU and TopK concept selectors.

JumpReLU concept selector. The JumpReLU activation function (Erichson et al., 2019) is defined as follows:

$$\text{JumpReLU}_{\mathbf{o}}(\mathbf{x}) = \mathbf{x} \cdot H(\mathbf{x} - \mathbf{o}) = \begin{cases} 0, & \mathbf{x} \leq \mathbf{o} \\ \mathbf{x}, & \mathbf{x} > \mathbf{o} \end{cases}, \quad (8)$$

where H is the Heaviside step function. Note that we cannot directly train our offset parameter \mathbf{o} . Thus, following Rajamanoharan et al. (2024), we used straight-through-estimators (Bengio et al.,

Table 3: **Overview of interpretable classifiers.** In the equations below, let $\tilde{s}(\mathbf{x}_i) := \text{sim}_{\mathbf{C}}(\mathbf{x}_i)$ denote the normalized cosine similarity between activations $\mathbf{a}_i = f(\mathbf{x}_i)$ for input \mathbf{x}_i and the concepts $\mathbf{C}, \mathbf{W} \in \mathbb{R}^{|\mathcal{Y}| \times |\mathbf{C}|}$ and $\mathbf{b} \in \mathbb{R}^{|\mathcal{Y}|}$ are the weights and bias of the linear classifier, $\mathbf{o} \in \mathbb{R}_+^{|\mathbf{C}|}$ is a trainable offset parameter, $y_i \in \mathcal{Y}$ denotes the target class of input \mathbf{x}_i for a total of $|\mathcal{Y}|$ classes, \mathcal{L} denotes the task-specific loss function (in our case cross-entropy loss throughout this work), R_α is the elastic net regularization penalty (Zou & Hastie, 2005), λ_w, λ_π govern the regularization strengths, H denotes the Heaviside step function, and TopK denotes the TopK activation function (Makhzani & Frey, 2014). Note that $\tilde{s}(\mathbf{x}_i)$ is frozen during optimization. Further, note that the TopK concept selector does not need a sparsity penalty since sparsity can be controlled directly using the parameter k .

name	concept selector π	interpretable classifier
ReLU	$\pi(\mathbf{x}_i) := \max(0, \tilde{s}(\mathbf{x}_i) - \mathbf{o})$	$\min_{\mathbf{W}, \mathbf{b}, \mathbf{o}} \sum_{i=1}^N \mathcal{L}(\mathbf{W}\pi(\mathbf{x}_i) + \mathbf{b}, y_i) + \lambda_w R_\alpha(\mathbf{W}) + \lambda_\pi R_\alpha(\pi(\mathbf{x}_i))$
JumpReLU	$\pi(\mathbf{x}_i) := \tilde{s}(\mathbf{x}_i) \cdot H(\tilde{s}(\mathbf{x}_i) - \mathbf{o})$	$\min_{\mathbf{W}, \mathbf{b}, \mathbf{o}} \sum_{i=1}^N \mathcal{L}(\mathbf{W}\pi(\mathbf{x}_i) + \mathbf{b}, y_i) + \lambda_w R_\alpha(\mathbf{W}) + \lambda_\pi \sum_j^{ \mathbf{C} } H(\tilde{s}_j(\mathbf{x}_i) - \mathbf{o}_j)$
TopK	$\pi(\mathbf{x}_i) := \text{TopK}(\tilde{s}(\mathbf{x}_i) - \mathbf{o})$	$\min_{\mathbf{W}, \mathbf{b}, \mathbf{o}} \sum_{i=1}^N \mathcal{L}(\mathbf{W}\pi(\mathbf{x}_i) + \mathbf{b}, y_i) + \lambda_w R_\alpha(\mathbf{W})$

Table 4: **Hyperparameter settings for all UCBMs variants on ImageNet — CUB — Places-365.**

	λ_π	k	λ_w	dropout rate
UCBM w/o concept selection	n/a	n/a		
UCBM with ReLU concept selector	2e-5 — 1e-4 — 2e-5	n/a	1e-4 — 8e-4 — 4e-4	0.1 — 0.2 — 0.2
UCBM with JumpReLU concept selector	1e-5 — 4e-7 — 4e-7	n/a		
UCBM with TopK concept selector	n/a	42 — 66 — 162		

2013) to make \mathbf{o} trainable. Specifically, we adopted the pseudo-derivates from Rajamanoharan et al. (2024):

$$\frac{\tilde{\partial}}{\partial \mathbf{o}} \text{JumpReLU}_{\mathbf{o}}(\mathbf{x}) := -\frac{0}{\epsilon} K\left(\frac{\mathbf{x} - \mathbf{o}}{\epsilon}\right) \quad (9)$$

and

$$\frac{\tilde{\partial}}{\partial \mathbf{o}} H(\mathbf{x} - \mathbf{o}) := -\frac{1}{\epsilon} K\left(\frac{\mathbf{x} - \mathbf{o}}{\epsilon}\right) \quad , \quad (10)$$

where $\tilde{\partial}$ denotes the pseudo-derivative, K is a kernel (following Rajamanoharan et al. (2024) we used the rectangle function: $\text{rect}(\mathbf{x}) := H(\mathbf{x} + \frac{1}{2}) - H(\mathbf{x} - \frac{1}{2})$), and ϵ can be seen as the KDE bandwidth.

TopK concept selector. The TopK activation function (Makhzani & Frey, 2014) is defined as follows:

$$\text{TopK}_k(\mathbf{x})_i = \begin{cases} \mathbf{x}_i & \text{if } \mathbf{x}_i \in \text{top-k}(\mathbf{x}), \\ 0 & \text{otherwise,} \end{cases} \quad (11)$$

Note that we can directly control the sparsity through the hyperparameter k and the TopK concept selector becomes equivalent to the identity function as $k = |\mathbf{C}|$.

Why do we add a trainable offset parameter \mathbf{o} ? We introduce the additional trainable offset parameter $\mathbf{o} \in \mathbb{R}_+^{|\mathbf{C}|}$ to allow the classifier to adapt to different ranges of alignment scores for each concept. The reasons for this is that the distribution of alignment scores can vary between concepts. For example, for one concept, the alignment scores may be more uniformly distributed, indicating a more ambiguous presence of the concept. For another concept, the alignment scores might follow a bimodal distribution, indicating two distinct modes that indicate the object is present or absent. The offset parameter helps the classifier in such cases to account for such different distributions.

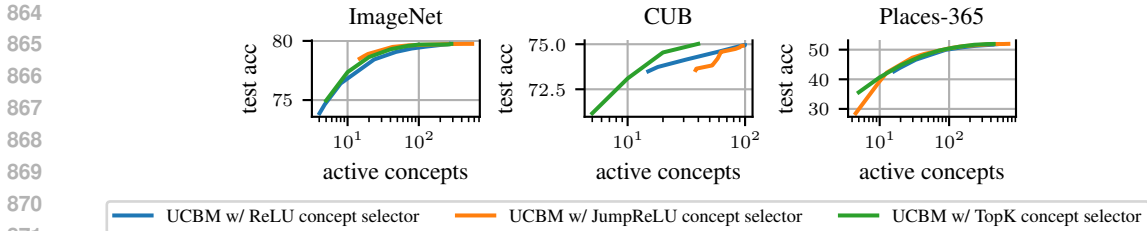


Figure 11: Trade-off curves between sparsity and performance of the three UCBM variants. We plot the mean number of active concepts per input according to Equation 7 as we decrease k (for TopK) or increase λ_π (for the others). Note that we only plot the Pareto-optimal points.

Table 5: UCBM with TopK concept selector requires less concepts to explain a prediction. We report the mean and the standard deviation of the number of concepts that are required to explain 95% of the prediction (see Equation 12 for more details).

Approach	#concepts to explain 95% of the prediction (Equation 12)		
	ImageNet	CUB	Places-365
UCBM w/o concept selection	9.51 ± 0.016	6.95 ± 0.05	46.12 ± 0.075
UCBM with ReLU concept selector	4.93 ± 0.002	5.93 ± 0.051	17.59 ± 0.031
UCBM with JumpReLU concept selector	6.27 ± 0.007	5.75 ± 0.099	28.53 ± 0.044
UCBM with TopK concept selector	6.15 ± 0.011	6.54 ± 0.041	28.22 ± 0.023

C HYPERPARAMETER SETTINGS

Table 4 provides the hyperparameters (λ_π , k , λ_w , dropout rate) for all our UCBMs variants. We chose those hyperparameters such that they yielded a good trade-off between performance, sparsity, and fair comparability (see Figure 4 and Appendices D and E). It is important to note that we first optimized λ_π for the ReLU and JumpReLU concept selectors and then set k accordingly, as we found that its relationship to sparsity (c.f., Equation 7) is straightforward.

D TRADE-OFF BETWEEN PERFORMANCE AND SPARSITY

The hyperparameter k for UCBM with TopK concept selector, or λ_π for UCBM with ReLU or JumpReLU concept selector, governs the model’s sparsity (c.f., Equation 7). It is important to note that this also affects performance—more sparse models typically have degraded performance. Figure 11 illustrates this trade-off. We find that each concept selector enables ‘smooth’ control over this trade-off. This allows practitioners to set these hyperparameters according to their desired balance between sparsity (and better interpretability) and performance, based on the requirements of their application.

Beyond the sparsity measurements and discussion for Table 2, we computed how many concepts the models need to explain their prediction of a class. For this, we computed the mean number of concepts that are required to explain 95% of a model’s prediction per sample:

$$\frac{1}{N} \sum_{i=1}^N C'_i, \text{ where } \min_{C'_i \subseteq \{1, \dots, |\mathbf{C}|\}} |C'_i| \text{ s.t. } \frac{\sum_{c \in C'_i} |\mathbf{W}_{\tilde{y}_i, c} \pi(\mathbf{x}_i)_c|}{\sum_{c \in \{1, \dots, |\mathbf{C}\}} |\mathbf{W}_{\tilde{y}_i, c} \pi(\mathbf{x}_i)_c|} \geq 95\% \quad , \quad (12)$$

where \tilde{y}_i denotes the model’s prediction of input \mathbf{x}_i .

Table 5 shows that UCBMs with concept selector rely on fewer concepts than UCBM without concept selection. Note that relying on fewer concepts makes it easier for users to comprehend a prediction since they do not need to inspect a lot of concepts.

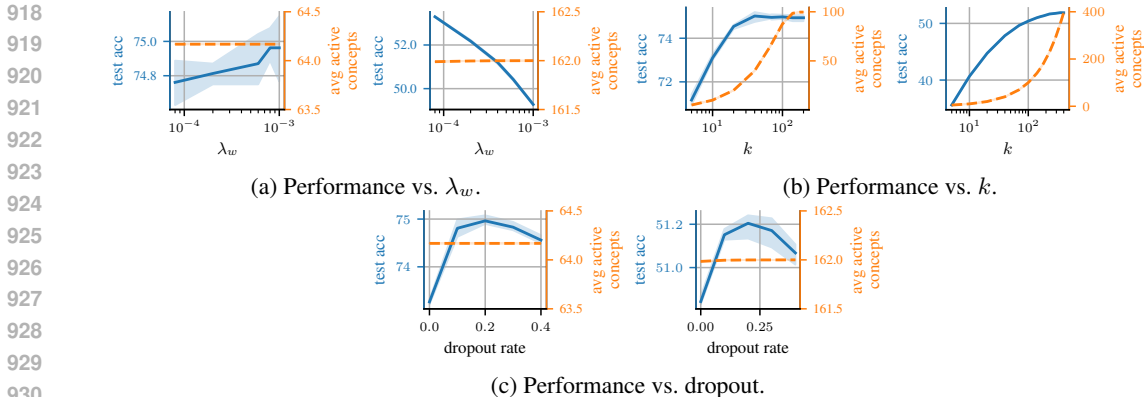


Figure 12: Sensitivity analysis for UCBM with TopK concept selector over λ_w (a), k (b), and the dropout rate (c) for CUB (left) and Places-365 (right).

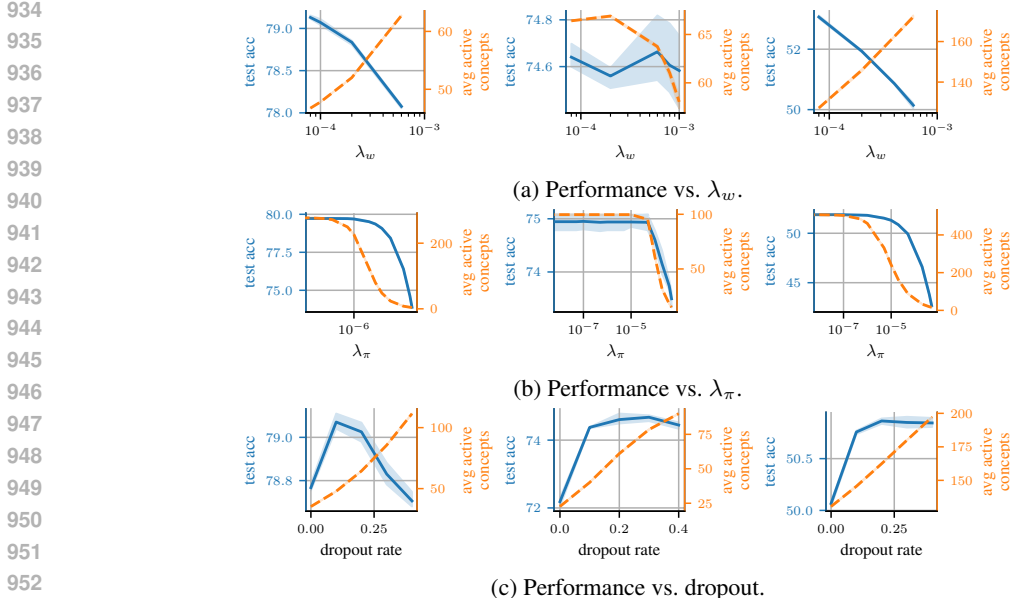


Figure 13: Sensitivity analysis for UCBM with ReLU concept selector over λ_w (a), λ_π (b), and the dropout rate (c) for ImageNet (left), CUB (middle), and Places-365 (right).

E ADDITIONAL SENSITIVITY ANALYSIS RESULTS

Figure 12 provides the results for the sensitivity analysis for UCBM with TopK concept selector on CUB and Places-365. Figures 13 and 14 provide the results for UCBM with ReLU or JumpReLU concept selector, respectively.

As also discussed in Appendix D, the hyperparameters k (for TopK) or λ_π (for ReLU and JumpReLU) control the trade-off between performance and sparsity. Regarding the other hyperparameters, λ_w and dropout rate, it is important to observe that they have less influence on the sparsity for the TopK concept selector than for the other concept selectors. We consider this as an advantage of the TopK concept selector, as it reduces the interaction between hyperparameters. This makes hyperparameter tuning simpler and simplifies the interpretation: k governs the average number of active concepts per sample, λ_w governs the number of concepts used per class, and the dropout rate influences whether the classifier relies on a broader or narrower set of concepts.

For λ_w , we find that increasing it typically leads to worse performance and a smaller average number of active concepts per sample. Interestingly, for the UCBMs with ReLU concept selector trained on

972
973
974
975
976
977
978
979
980
981
982
983
984
985
986
987
988
989
990
991
992
993
994
995
996
997
998
999
1000
1001
1002
1003
1004
1005
1006
1007
1008
1009
1010
1011
1012
1013
1014
1015
1016
1017
1018
1019
1020
1021
1022
1023
1024
1025

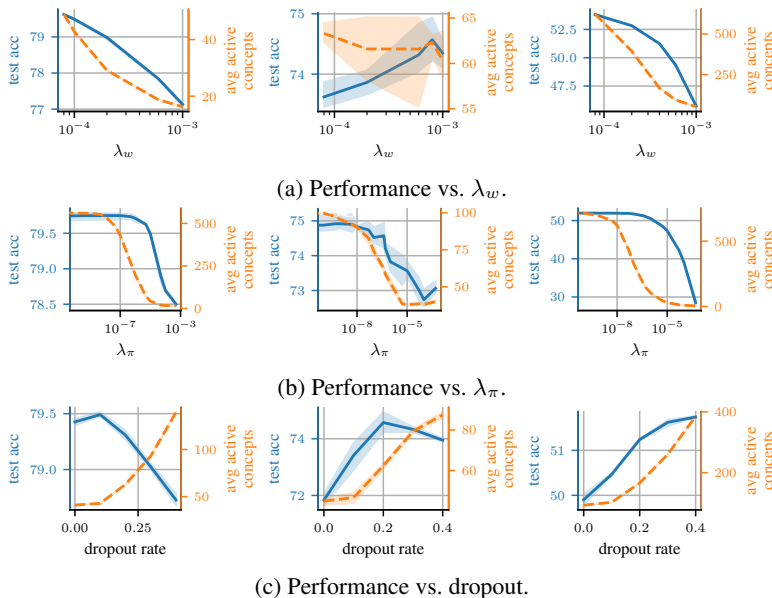


Figure 14: Sensitivity analysis for UCBM with JumpReLU concept selector over λ_w (a), λ_π (b), and the dropout rate (c) for ImageNet (left), CUB (middle), and Places-365 (right).

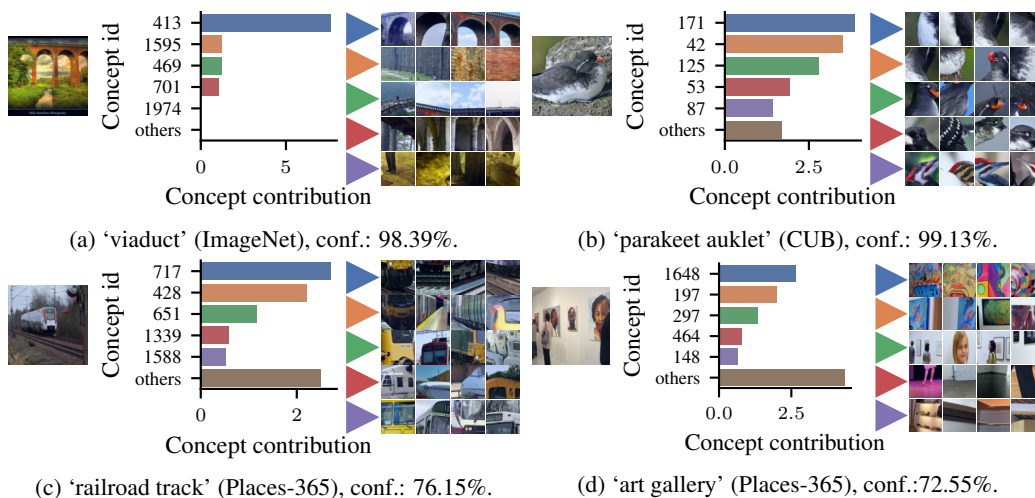


Figure 15: Explainable decisions by UCBM with TopK concept selector on ImageNet (a), CUB (b), and Places-365 (c, d) classes. The model’s prediction are comprehensible and typically rely on only few concepts.

ImageNet and Places-365, we observe the opposite behavior. For the dropout rate, a higher dropout rate results in more active concepts per sample, though its relationship with performance is less straightforward.

F ADDITIONAL EXAMPLES OF EXPLAINABLE DECISIONS

Additional examples for sample-wise explanations. Figure 15 provides more examples of explainable decision of UCBM with TopK concept selector on ImageNet, CUB, and Places-365. We typically find that our method relies on a small set of concepts that are present in the images, human-comprehensible and class-relevant. For instance, for the viaduct in Figure 15a, UCBM uses class-relevant concepts (e.g., ‘arches’, ‘stones’, or ‘walkway’). For the ‘railroad track’ in Figure 15c, it

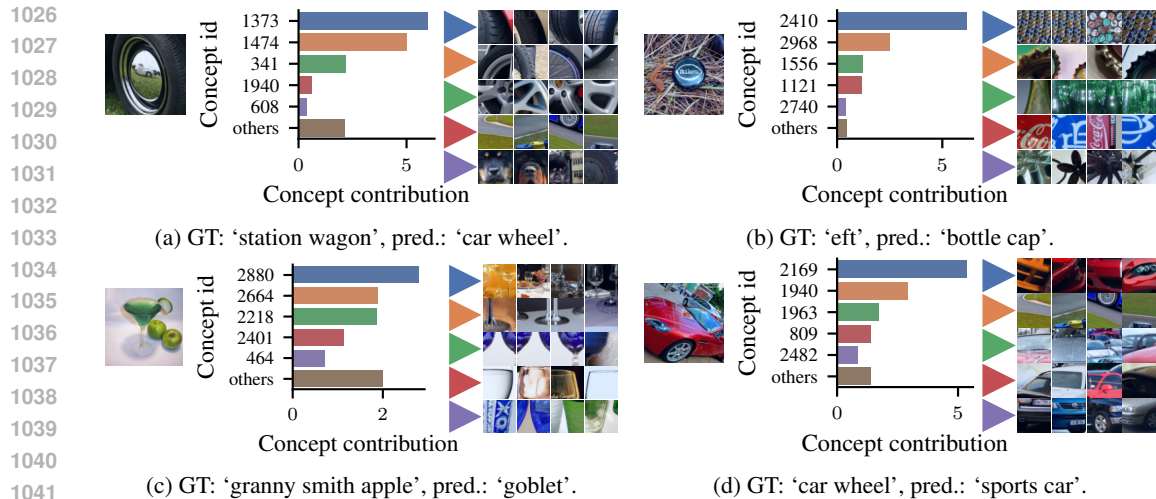


Figure 16: **The most contributing concepts explain the misclassifications on ImageNet of UCBM with TopK concept selector.** **a:** The image shows a station wagon mirrored in a car wheel. Most of the top-5 concepts are related to car wheels, which explains that the model only focuses on the car wheel itself instead of the mirrored station wagon. This clearly explains why the model predicts 'car wheel' instead of 'station wagon'. **b:** The image shows an eft next to a bottle cap. The concepts show that the model used concepts related to bottle caps, which is the object at the center of the image. **c:** The image shows two granny smith apples next to a goblet that was predicted by the model. The concepts reveal that the model focuses on concepts related to the goblet at the center of the image. **d:** The image shows a sports car, including one of its front wheels. The most important concept is related to sports cars. The other concepts also focus more on general car concepts than on the wheels.

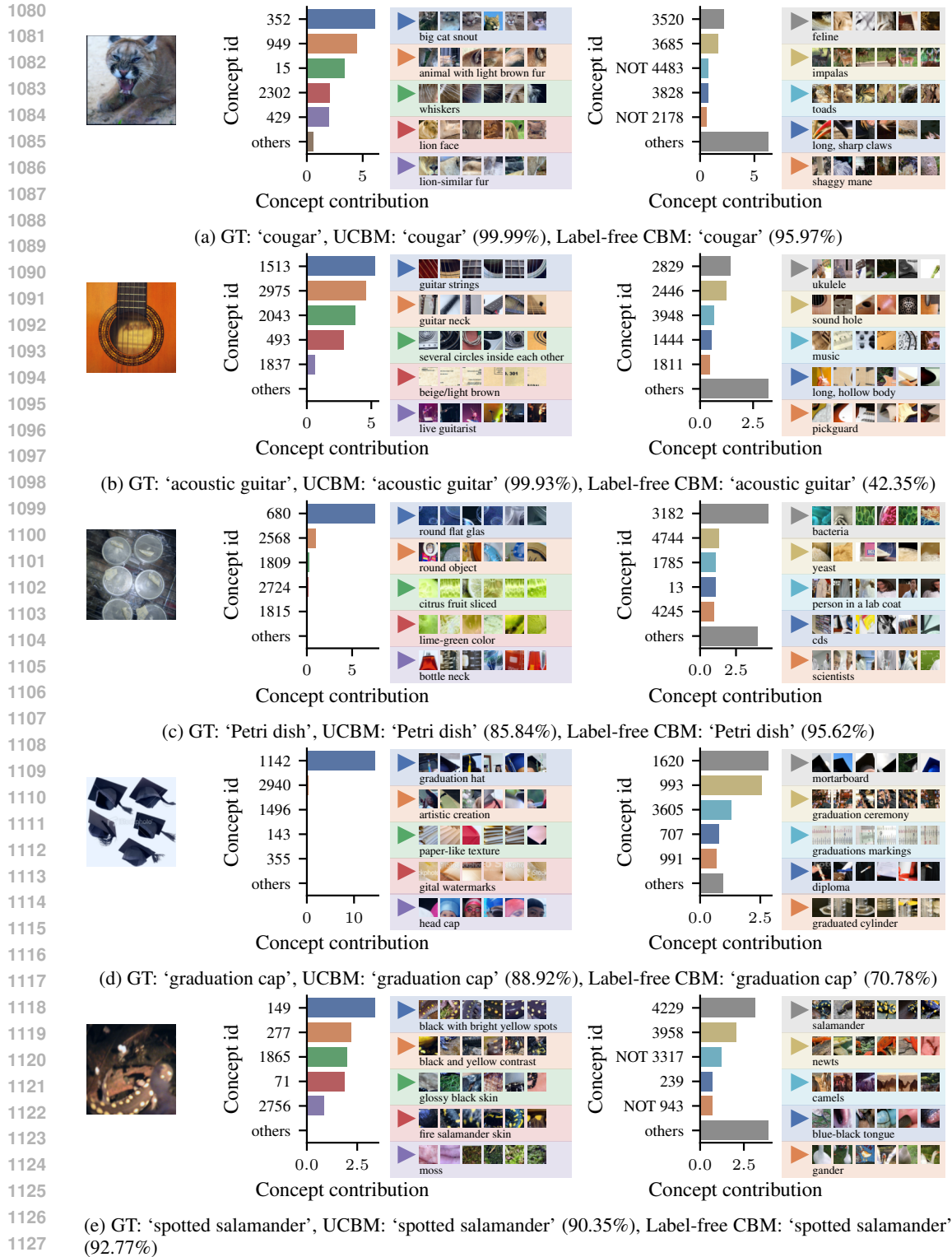
uses concepts such as 'tracks' or 'train'. Interestingly, it also uses the concept 'large window' that is also related to, e.g., buses. This indicates that UCBMs first assess if concepts are present or absent and then based on that evidence predict the class that is most likely given that.

Understanding misclassifications of UCBMs. Figure 16 shows that we can comprehend why UCBMs made a misclassification. For example, Figure 16a shows that the UCBM incorrectly predicted 'car wheel' instead of 'station wagon'. However, the image shows such station wagon mirrored in a car wheel. Looking at the most contribution concepts reveals that UCBM focused on concepts that are related to the car wheel, as it is the most salient in the image.

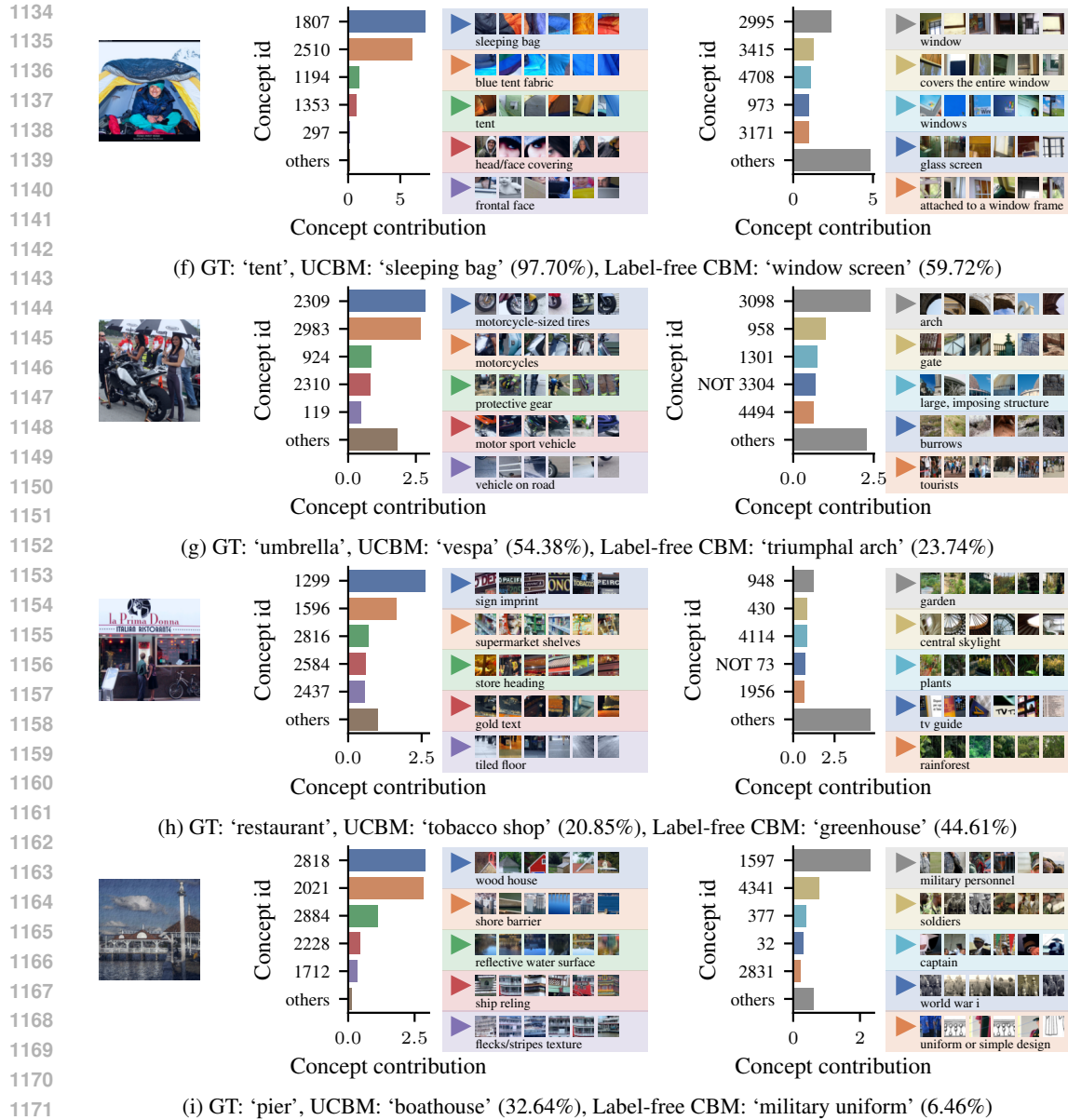
Additional examples for the comparison of UCBM to Label-free CBM. Figure 17 compares the explanations of UCBM with TopK concept selector and Label-free CBM (Oikarinen et al., 2023). We find that our approach provides more comprehensible explanations:⁵ UCBM relies on intuitive concepts that are present in the image and relevant to the prediction. In contrast, Label-free CBM tends to rely on concepts that are correlated to the prediction but may not be present in the image, e.g., the concepts 'graduation markings' or 'diploma' for the prediction 'graduation cap' in Figure 17d.⁶ Note that such reliance on prediction-class correlated but absent concepts is particularly pronounced for misclassifications (Figures 17f to 17i). For example, Label-free CBM relies on the concepts 'garden', 'plants', or 'rainforest' for an image that depicts an restaurant from the street (without any greenery). We believe relying on such non-visible concepts is not helpful to understand the decision of a concept-based model.

⁵These qualitative findings are further corroborated in the user study in Section 3.2 and Appendix G.

⁶We suspect the reason for this are shortcomings of CLIP's embeddings. For instance, the concepts 'graduated cylinder' is unrelated to the prediction of 'graduation cap' in Figure 17d. However, the word 'graduated' is related to 'graduation'. Indeed, when we compute the cosine similarity of text features (we considered the following: 'graduated cylinder', 'graduation ceremony', 'graduation markings', 'graduation', 'university', 'dog', 'house'), we found that concepts related graduation have higher similarities with the graduated cylinder than the unrelated concepts. We leave further investigations for future work.



Besides that, we find that a significant part of the concept contributions of the decisions of Label-free CBM is also attributed to other concepts (bar 'others' in the plots). In contrast, UCBMs typically rely on fewer concepts. The benefit of this is that users have to only consider a small set of concepts in practice, making the interpretability of UCBMs' explanations easier to comprehend.



1172
1173
1174
1175
1176
1177
1178
1179

Figure 17: **Comparison of explainable decisions of UCBM with TopK concept selector (left) vs Label-Free CBM (right).** Subfigures a-e and f-i show correct or incorrect predictions of both CBMs, respectively. Our UCBM with TopK concept selector provides more comprehensible explanations, while Label-free CBM often relies on concepts that are not even visible in the image (this is especially pronounced for misclassifications). We suspect one reason for this are the shortcomings of CLIP’s text features that are used in Label-free CBM.

1180 G FURTHER DETAILS ON THE USER STUDY

1181
1182
1183
1184
1185

In the user study, we studied whether users consider the explanations of the decisions of UCBM to be comprehensible. To do so, we compared the explanations of UCBM with TopK concept selector with Label-free CBM (Oikarinen et al., 2023). Both were trained on ImageNet.

1186
1187

Task. We asked users to assess which model provides a more comprehensible explanation from a scale from ‘Model A clearly more’ to ‘Model B clearly more’. Further, we asked for the reasons why they think one model is more comprehensible than the other.

1188
1189
1190
1191
1192
1193
1194
1195
1196
1197
1198
1199
1200
1201
1202
1203
1204
1205
1206
1207
1208
1209
1210
1211
1212
1213
1214
1215
1216
1217
1218
1219
1220
1221
1222
1223
1224
1225
1226
1227
1228
1229
1230
1231
1232
1233
1234
1235
1236
1237
1238
1239
1240
1241

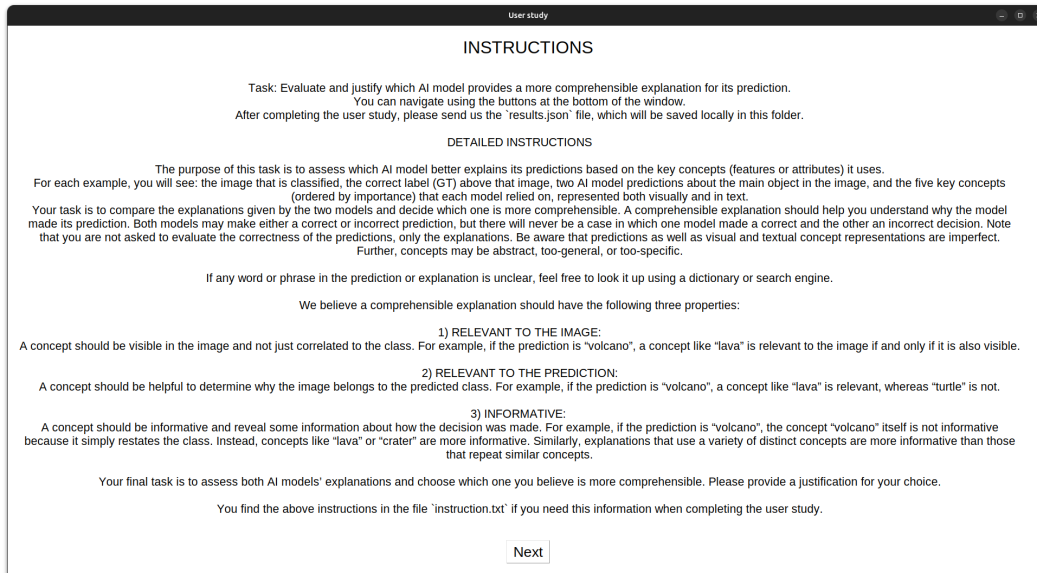


Figure 18: Instruction text.

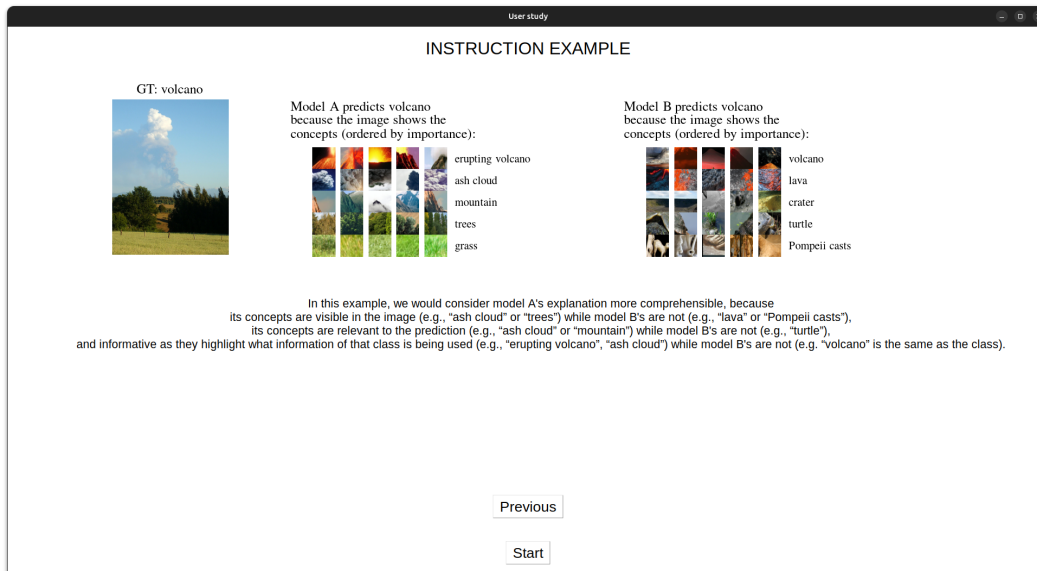


Figure 19: Instruction example.

User study data. We showed users local explanations based on which concepts contributed the most to the decision of each model, akin to Figures 6, 8, 15 and 16. Importantly, 20% of samples showed misclassifications of *both* models (for the other 80% both model predicted correctly).⁷ We include misclassifications to also understand how comprehensible models are under errors. We believe this is an important aspect to study, as users will also interact with models that make errors in practice. For sake of this user study, we simplified the explanations by removing the concept contributions and only showed the names and top-activating image crops of the five most contributing concepts and a corresponding concept description.

Note that UCBM and Label-free CBM represent their concepts differently: UCBMs show visual representations, whereas Label-free CBM shows concept descriptions. To ensure fair comparison,

⁷No sample for which one model was correct and the other was incorrect was shown in the user study.

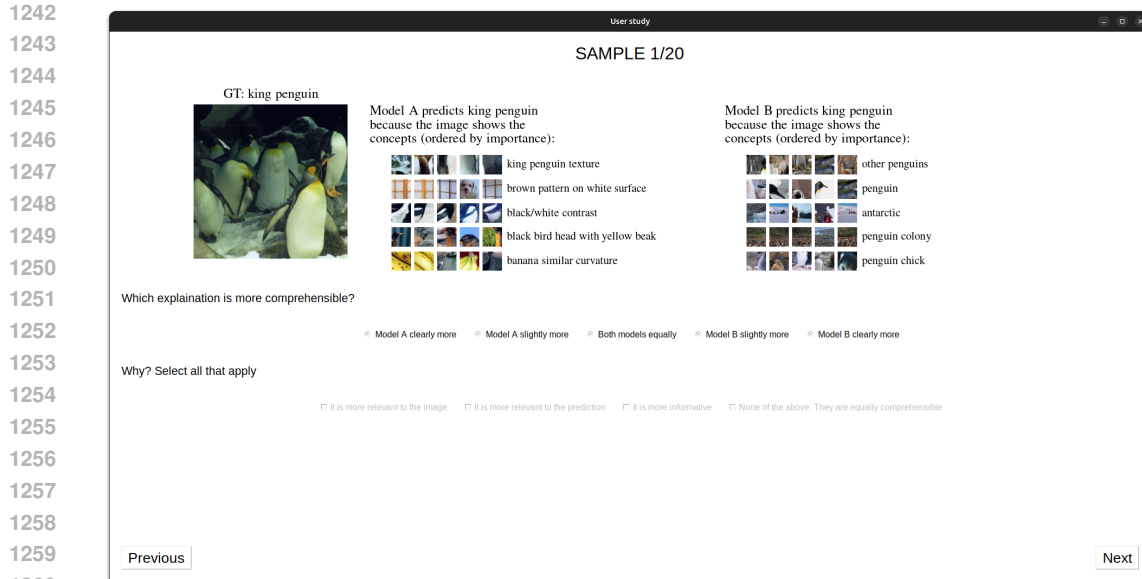


Figure 20: User study sample.

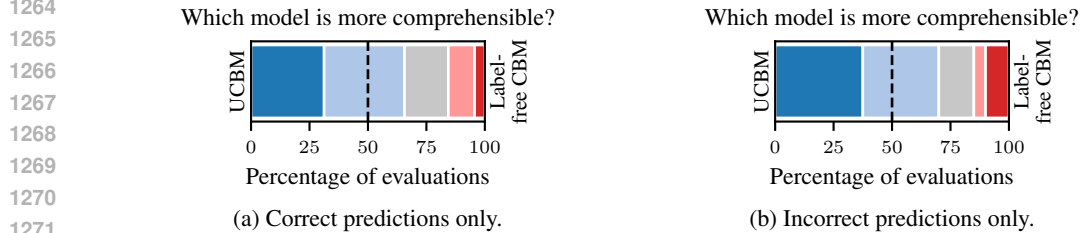


Figure 21: Users strongly preferred UCBM with TopK concept selector over Label-free CBM for correct as well as incorrect predictions.

1272
1273
1274
1275
1276

1277 we labeled the most activating image crops of UCBM’s concepts and retrieved images using SigLIP
1278 SoViT-400m (Zhai et al., 2023; Alabdulmohsin et al., 2023) for Label-free CBM’s concepts.
1279

1280
1281 **Setup.** We implemented the user study in a lightweight Python GUI so that users could run the
1282 study locally on their machine. Users were provided with the task description (Figure 18) and an
1283 example (Figure 19). After the instruction, users interacted with our user study interface (Figure 20).
1284

1285 We asked ten users to rate a total of 200 samples (20 per user). Users participated voluntarily and
1286 without payment. They have strong background in machine learning and related fields. However,
1287 none of them is working on concept-based models or had seen explanations of UCBM before.
1288

1289
1290 **Further analysis.** Complementary to the results presented in Section 3.2, we conducted further
1291 analysis on the results of the user study. Figure 21 shows that users strongly preferred our UCBM
1292 with Topk concept selector over Label-free CBM in ca. 65-70% of evaluations (Label-free CBMs
1293 are only preferred in ca. 15%). Users’ preference was similar for correct or incorrect predictions.

1294 Users based their preference decisions mostly on relevance to the prediction (selected in 66.5% of the
1295 evaluations). However, relevance to the image (55%) and informativeness (55%) closely followed
it.

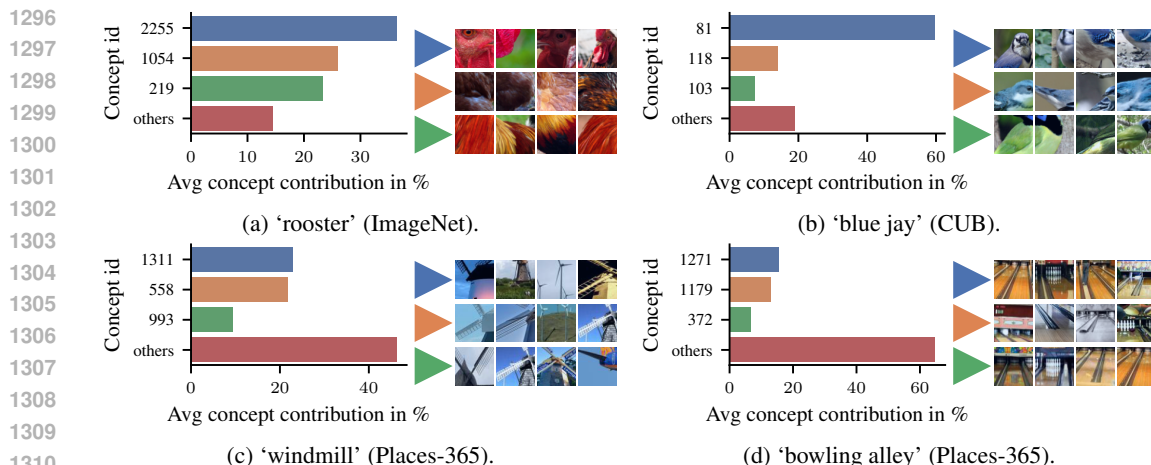


Figure 22: **Visualization of decision rules learned by UCBM with TopK concept selector on ImageNet (a), CUB (b) and Places-365 (c, d).**

H ADDITIONAL EXAMPLES OF EXPLAINABLE DECISION RULES

Figure 22 provides more examples of explainable decision rules of UCBM. The examples show that UCBM uses reasonable human-interpretable concepts to build the score of a specific class.

I CONCEPT LABELING WITH A LARGE VISION-LANGUAGE MODEL

As an alternative to providing the top-activating image crops and manual concept labelling, we also experimented with large vision-language models (GPT-4o (Achiam et al., 2023)) to automatically label concepts. We prompted it with the top-9 image crops and task description:

*The nine pictures within the image are matching a specific concept.
Can you describe the concept with very few words (ca. 1–3)?*

Figure 23 shows the outputted concept labels for twelve, diverse concepts. Overall, we found that concept labels are mostly matching to the top image crops, e.g., Figures 23a, 23d, 23e and 23k. However, there are also instances that may not be correctly labelled. For example, the large vision-language model outputs “motorcycle racing” for the image crops in Figure 23b. While this matches well with most of the image crops, it does not for the baseball player (bottom middle) and cyclist (bottom right). We suspect that the concept is representing a more general concept for “safety equipment” instead. For another example, in Figure 23h, the large vision-language model labelled the concept as “ocean textures”. However, the image crops more likely resemble a starry sky rather than some ocean textures due to the point structure.

J EXAMPLE PROMPT TO THE LARGE VISION-LANGUAGE MODEL

Figure 24 shows an example prompt to the large vision-language model for the misclassification from the lower, left subfigure in Figure 9. Figure 25 shows the corresponding output from the large vision-language model.

1350
 1351
 1352
 1353
 1354
 1355
 1356
 1357
 1358
 1359
 1360
 1361
 1362
 1363
 1364
 1365
 1366
 1367
 1368
 1369
 1370
 1371
 1372
 1373
 1374
 1375
 1376
 1377
 1378
 1379
 1380
 1381
 1382
 1383
 1384
 1385
 1386
 1387
 1388
 1389
 1390
 1391
 1392
 1393
 1394
 1395
 1396
 1397
 1398
 1399
 1400
 1401
 1402
 1403

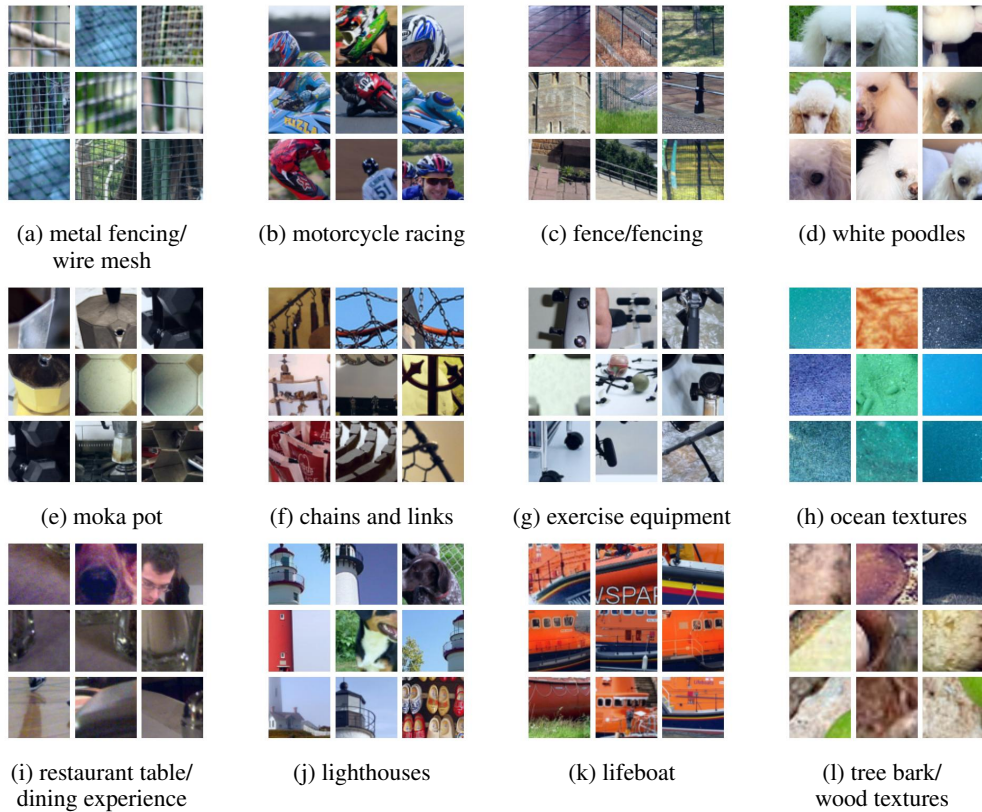


Figure 23: **Labeling of concepts using large vision-language models.** The subfigures’ captions are the labeling/descriptions that the large vision-language model (GPT-4o (Achiam et al., 2023)) assigned to the provided concept visualizations.

1404
1405
1406
1407
1408
1409
1410
1411
1412
1413
1414
1415
1416
1417
1418
1419
1420
1421
1422
1423
1424
1425
1426
1427
1428
1429
1430
1431
1432
1433
1434
1435
1436
1437
1438
1439
1440
1441
1442
1443
1444
1445
1446
1447
1448
1449
1450
1451
1452
1453
1454
1455
1456
1457



The image from above leads to the following output if we are putting it into a trained concept bottleneck model.

Ground truth: tench
Prediction: eel

Top-5 model prediction sorted by the logits:

Class eel: 7.71
Class tench: 7.05
Class silver salmon: 6.76
Class snoek fish: 6.08
Class sturgeon: 5.93

Largest five concept contributions (by absolute value) for ground truth class tench, sorted by size (and their weight in the final linear layer):

Concept 2088: 5.27 (0.34)
Concept 2987: 1.48 (0.20)
Concept 162: 0.17 (0.01)
Concept 2177: 0.01 (0.00)
Concept 2479: 0.01 (0.00)

Largest five concept contributions (by absolute value) for predicted class eel sorted by size (and their weight in the final linear layer):

Concept 333: 2.94 (0.34)
Concept 1367: 2.26 (0.20)
Concept 760: 0.72 (0.11)
Concept 2088: 0.68 (0.04)
Concept 2987: 0.51 (0.07)

Furthermore, the layer from the concept similarities to the prediction is a linear layer. Which weights (concept and class) should be adjusted by how much in order to get a correct classification for this image, while not changing any other classifications? Please give an answer in case of 'increase/decrease weight of class i and concept j by x '.

Figure 24: Input prompt to the large vision-language model to edit the linear classifier’s weights to correct an error.

1458
 1459
 1460
 1461
 1462
 1463
 1464
 1465
 1466
 1467
 1468
 1469
 1470
 1471
 1472
 1473
 1474
 1475
 1476
 1477
 1478
 1479
 1480
 1481
 1482
 1483
 1484
 1485
 1486
 1487
 1488
 1489
 1490
 1491
 1492
 1493
 1494
 1495
 1496
 1497
 1498
 1499
 1500
 1501
 1502
 1503
 1504
 1505
 1506
 1507
 1508
 1509
 1510
 1511

To get the model to correctly classify the image as "tench" instead of "eel," we'll need to adjust the weights in the final linear layer between the relevant concepts and the classes. Here's the approach to identifying which weights should be adjusted and by how much:

Step-by-step Approach:

1. Identify Misclassification and Concept Contributions:
 - The model currently predicts "eel" with a logit of 7.71, while "tench" has a logit of 7.05.
 - To change the classification to "tench," we need the logit for "tench" to be higher than the logit for "eel."
2. Calculate Difference Needed:
 - Currently, the difference between "eel" and "tench" logits is: $7.71 - 7.05 = 0.66$.
 - To correctly classify the image as "tench," the logit for "tench" must exceed "eel." Therefore, we need to adjust the weights such that the logit for "tench" increases by at least 0.66.
3. Determine Which Concept Weights to Adjust:
 - For "tench," the largest contributing concept is 2088 with a contribution value of 5.27 and a weight of 0.34.
 - For "eel," concept 2088 is also present with a smaller contribution (0.68) and a lower weight (0.04).
 - Adjusting concept 2088's weight for "tench" might be the most straightforward way to change the output because it has a significant contribution value.
4. Calculate Weight Adjustments:
 - To increase the "tench" logit by 0.66, we need to find an increase in the weight of concept 2088 for "tench":

$$\text{Increase in logit} = \text{concept contribution} \times \text{weight increase.}$$

Here, the concept contribution for 2088 is 5.27. So, we need to find the weight increase (Δw) such that:

$$5.27 \times \Delta w = 0.66.$$

Solving for Δw :

$$\Delta w = \frac{0.66}{5.27} \approx 0.125$$

5. Adjust the Weight:
 - Increase the weight between "tench" and concept 2088 by approximately 0.125.

Final Answer:

- Increase the weight of class tench and concept 2088 by 0.125.

This targeted adjustment will help correct the classification for this specific image without affecting other classifications significantly, as it focuses on the concept that most strongly contributes to the "tench" logit.

Figure 25: Output of the large vision-language model to edit the linear classifier's weights to correct the error.